

## Response to reviewer #1

Thank you for the comprehensive comments, and also for taking the time to truly read through our manuscript. We feel that your comments were very helpful for increasing the quality of the paper to its current level. Your comments, together with those of referee #2, led to a thorough revision of the paper.

5 The most general comments regarding the revisions to the manuscript are:

1. Due to the maize cropland at Yangling station was irrigated and the maize was not suffered severe water and heat stress, a grassland, which experienced severe drought at Vaira Ranch (US-Var) Fluxnet site, was used to validate the ability of STEMMUS-SCOPE responding to drought.
2. Some figures and tables were changed. We updated Table 1 because the previous table ignored the latest improvements in some LSMs. We added the Table 2 for presenting the difference among SCOPE, SCOPE\_SM, STEMMUS, and STEMMUS-SCOPE. The figure of root length density was changed into a table for comparing simulated root length density and observed that in different sites.
3. We presented modeled half-hourly transpiration, gross primary production, solar-induced fluorescence, and leaf water potential and analyzed the relationship among gross primary production, solar-induced fluorescence, and leaf water potential.
4. We added a new section for discussing the advanced plant hydraulics and root growth processes and what STEMMUS-SCOPE needs to be improved in the next step. Besides, we have tried to enhance the structure in the revised manuscript.

The reviewers' comments are in black and [our responses in blue](#).

Main concerns:

- 20 **Comments 1:** *SCOPE is a vertical (1-D) integrated radiative transfer and energy balance model, which is widely used in the simulations of vegetation photosynthesis process and fluorescence at the leaf and canopy level. The soil model is very simplified in SCOPE. It is interesting to see the STEMMUS Model, which is good at dealing with the mass and heat transfer processes in unsaturated soil, is implemented into SCOPE. However, I do not see significant improvements in the SCOPE\_STEMMUS model in current manuscript, although the SCOPE\_STEMMUS includes root water uptake in unsaturated soil. I think this*
- 25 *shortcoming lies in the model validations based on the measurements at the Yangling station. As we know, SCOPE model has*

the abilities to simulate the vegetation photosynthesis and evapotranspiration under the unstressed water conditions (Zhang et al., 2020; Shan et al., 2019; Zhang et al., 2018). And the Yangling station has irrigation and vegetation growth do not have water and heat stresses in 2017. Therefore, we can see very similar simulations from SCOPE and SCOPE\_STEMMUS in Figure 6 and 7, which means the similar ability of SCOPE\_STEMMUS and SCOPE in simulating ET and T. I think more sites that have water or heat stresses should be used for the validations to prove the better ability of SCOPE\_STEMMUS.

**Response:** Thanks for the constructive comment! The authors added a new validation at a grassland which was the same FLUXNET site used in Bayat's paper. The advantage of STEMMUS-SCOPE can be seen obviously in the simulation at grassland, especially when the vegetation experiencing moderate water stress. The reason is that STEMMUS-SCOPE considered root length density and soil water content distribution in the root zone. However, SCOPE\_SM could overestimate or underestimate the effect of water stress due to it only using the soil water content at a specific soil depth or average root zone soil moisture. For the grassland, when the dry season coming, the surface soil was very dry, and grass root can absorb deep soil water to meet the high transpiration rate. So, it is not reasonable using the soil water content at 10 cm depth to calculate water stress factor. For the maize cropland, as we use the averaged root zone soil water content as the input of SCOPE\_SM, the model will underestimate the effect of drought. The reason is that the maize root was concentrated at 20 cm to 40cm soil depth. The higher water content in deep soil cannot be fully used by maize in SCOPE-SM because of the less root distribution in deep soil. Furthermore, the authors are working on validating the coupled model at more different ecosystem. The current paper is focused on model development (Page 28, line 319-325; Page 32, line 380-388)

**Comments 2:** For the development of SCOPE model, Bayat et al. (2019) have extended the SCOPE model to combine optical reflectance and soil moisture observations for remote sensing of ecosystem functioning under water stress conditions. Bayat's work has overcome the shortcoming in biased estimations of GPP and ET under water stressed conditions and the significant improvements of GPP and ET in SCOPE\_SM model have shown in the paper. We also see the same abilities of SCOPE\_SM and SCOPE\_STEMMUS in simulating ET in this manuscript. Therefore, the authors should declare what the improvements are in SCOPE\_STEMMUS model. Terrestrial biosphere models typically use empirical functions to represent vegetation responses to soil drought, especially in the water-limited areas. These functions largely neglect recent advances in plant ecophysiology that link xylem hydraulic functioning with stomatal responses to climate. I think this may be a direction to declare the new insights in the impacts of water stress on the vegetation growth, due to the descriptions of root water uptake in STEMMUS model.

55 **Response:** Although Bayat et al. (2019) have extended the SCOPE model to combine optical reflectance and soil moisture observations for remote sensing of ecosystem functioning under water stress conditions, the distribution of fine root and soil moisture were ignored. For the very wet or very dry condition, the soil moisture at a specific depth can not reflect the water content in the whole root zone and the root water uptake was not sensitive to root distribution. But when the vegetation suffering moderate water stress, the hydraulic redistribution (RH) process and compensatory root water uptake (CRWU) process enable the plant absorb more water in the (deeper) soil layer with high soil water content, which were not taken account in SCOPE\_SM. These two processes were sensitive to vertical distribution of root system and soil moisture. These  
60 considerations enabled STEMMUS-SCOPE perform better when the grass site transited from wet season to dry season. Therefore, the coupled model accurately characterized the effect of moderate stress. The model can also be easily extended to include more plant hydraulics related plant traits but is beyond the scope of the current paper (Page 32, line 380-388)

*Comments 3: In Table 1, some information should be updated. Nowadays, CLM5.0, CALBLE and JULES have large improvements in the hydraulic functioning with stomatal responses to the warming climate (De Kauwe et al., 2020; Lawrence et al., 2020; Eller et al., 2020). And the authors should have more discussion about the root water uptake and the hydraulic functioning in the SCOPE\_STEMMUS model in this manuscript.*

70 **Response:** Thank you for sharing these useful references! As this study was conducted in 2019, some update in these LSMs was not included in the previous manuscript. In this version, we updated the latest improvements in CLM5.0, CALBLE, Noah-MP, and JULES (Table 1). In addition, some discussion about hydraulic function was added (Section 3.8: Page 39, line 482-518).

*Comments 4: The quality of some figures should be improved. This paper focus on the model developments and the better ability of the new model should be clear to the readers. For example, Figure 2 should be removed to the supplemental material. And Figure 5 and 8 are difficult for the readers to see and these figures should be redraw.*

**Response:** Figure 2 was changed and the data description can be found in references. Besides, figure 5 and 8 were redrawn.

## 75 **Response to reviewer #2**

Thank you for the comprehensive comments. Your comments, together with those of referee #1, led to a thorough revision of the paper.

The most general comments regarding the revisions to the manuscript are:

1. Due to the maize cropland at Yangling station was irrigated and the maize was not suffered severe water and heat stress, a grassland, which experienced severe drought at Vaira Ranch (US-Var) Fluxnet site, was used to validate the ability of STEMMUS-SCOPE responding to drought.  
80
2. Some figures and tables were changed. We updated Table 1 because the previous table ignored the latest improvements in some LSMs. We added the Table 2 for presenting the difference among SCOPE, SCOPE\_SM, STEMMUS, and STEMMUS-SCOPE. The figure of root length density was changed into a table for comparing simulated root length  
85 density and observed that in different sites.
3. We presented modeled half-hourly transpiration, gross primary production, solar-induced fluorescence, and leaf water potential and analyzed the relationship among gross primary production, solar-induced fluorescence, and leaf water potential.
4. We added a new section for discussing the advanced plant hydraulics and root growth processes and what STEMMUS-  
90 SCOPE needs to be improved in the next step. Besides, we have tried to enhance the structure in the revised manuscript.

The reviewers' comments are in black and [our responses in blue](#).

Main concerns:

*Comments 1: It was difficult to see what are overarching scientific question and findings (including development of a novel model) in the current manuscript. Although the authors mentioned “most of the current vegetation photosynthesis models do not account for root water uptake, which compromises their applications under water, stressed conditions (PIL15-)”, it should be noted that there are numerous SPAC models that are successful in taking into consideration the root water uptake (the authors should look at the pioneer paper (Williams et al. 1996, PCE 19, 911-927)). I think all figures shown in this manuscript can be reproduced by most existing SPAC models including most DGVMs, and thus, I feel they are meaningless to be represented.*  
95

100 *Frankly speaking, because of the above reason I feel the current manuscript cannot be reviewed anymore, but I also feel this work is very potential. I acknowledge SCOPE has a huge advantage in terms of calculation of leaf-scale chlorophyll fluorescence. Thus, as the authors mentioned at the end of the manuscript (P21L392-), SCOPE\_STEMMUS can be very state-of-the-arts SPAC model that can simulate the effect of plant water stress via soil moisture status on leaf-to-canopy scale chlorophyll fluorescence.*

105 *Thus, I will reject the current manuscript temporarily, but I strongly encourage the authors to resubmit this work with adding modelling results and discussion about the effect of plant water stress via soil moisture status on leaf-to-canopy scale chlorophyll fluorescence, which might be easily simulated using SCOPE\_STEMMUS. For this, the authors should note: Obviously SCOPE\_STEMMUS failed to reproduce the root developments (Fig. 12), but is successful in reproduction of transpiration and NEE. This is a serious inconsistency that prevents sound simulations of the effect of water stress on leaf gas*  
110 *exchange, and must be solved for resubmitting this work.*

**Response:** Indeed, SCOPE has a huge advantage in terms of calculation of leaf-scale chlorophyll fluorescence (*SIF*). We have added and compared the simulated *SIF* of SCOPE, SCOPE\_SM, and STEMMUS-SCOPE, and analyzed the relationship between *SIF* and leaf water potential (*LWP*). In addition, the authors are sorry for not presenting the simulation of root length density clearly in the previous manuscript. Actually, STEMMUS-SCOPE well simulated root growth. The simulated root  
115 length density (*RLD*) was comparable to the measurements from sites from Beijing, China, Potenza, Italy, and Tokyo, Japan. These lines were shaded by the simulated *RLD* by STEMMUS-SCOPE in the previous figure. In the revised manuscript, the authors changed Figure 12 into a table which can present simulated *RLD* more clearly. (Page 37, line 448-474)

**Comments 2:** *Though this is trivial point compared to the above-mentioned, I assumed the first author is an inexperienced scientist. For example, there was an ambiguous definition between “Results” and “Discussion” sections and were many wrong*  
120 *wordings. So I recommend to resubmit your paper to academic journals after thorough checking by the other experienced authors.*

**Response:** Thanks for your comment. The manuscript has been reconstructed and modified by senior authors.

## Response to executive editor

*In my role as Executive editor of GMD, I would like to bring to your attention our Editorial version 1.2:*

125 *<https://www.geosci-model-dev.net/12/2215/2019/> This highlights some requirements of papers published in GMD, which is also available on the GMD website in the 'Manuscript Types' section:*

*[http://www.geoscientific-model-development.net/submission/manuscript\\_types.html](http://www.geoscientific-model-development.net/submission/manuscript_types.html)*

*In particular, please note that for your paper, the following requirements have not been met in the Discussions paper:*

• *"The main paper must give the model name and version number (or other unique identifier) in the title."*

130 • *"If the model development relates to a single model then the model name and the version number must be included in the title of the paper. If the main intention of an article is to make a general (i.e. model independent) statement about the usefulness of a new development, but the usefulness is shown with the help of one specific model, the model name and version number must be stated in the title. The title could have a form such as, "Title outlining amazing generic advance: a case study with Model XXX (version Y)"."*

135 *As SCOPE is the model to which all your modifications and evaluation applies, SCOPE and a unique identifier, for the resulting version after integration of your modifications, should be named in the title of your article in your revised submission to GMD.*

**Response:** Thanks, Astrid Kerkweg, for your comments! We added the name of the coupled model to the title in this revised manuscript.

# 140 Integrated ~~Modeling~~Modelling of Canopy Photosynthesis, Fluorescence, and the Transfer of Energy, Mass and Momentum in the Soil-Plant-Atmosphere Continuum System(STEMMUS-SCOPE v1.0.0)

145 Yunfei Wang<sup>a, b, c, e</sup>, Yijian Zeng<sup>c</sup>, Lianyu Yu<sup>c</sup>, Peiqi Yang<sup>c</sup>, Christiaan Van der Tol<sup>c</sup>, Qiang Yu<sup>e</sup>, Xiaoliang Lü<sup>e</sup>, Huanjie Cai<sup>a, b, \*</sup>, Zhongbo Su<sup>c, d, \*</sup>,

<sup>a</sup> College of Water Resources and Architectural Engineering, Northwest Agriculture and Forestry University, Yangling, China

<sup>b</sup> Institute of Water Saving Agriculture in Arid Regions of China (IWSA), Northwest Agriculture and Forestry University, Yangling, China

<sup>c</sup> Faculty of Geo-Information Science and Earth Observation, University of Twente, Enschede, the Netherlands

150 <sup>d</sup> Key Laboratory of Subsurface Hydrology and Ecological Effect in Arid Region of Ministry of Education, School of Water and Environment, Chang'an University, Xi'an, China

<sup>e</sup> State Key Laboratory of Soil Erosion and Dryland Farming on the Loess Plateau, Institute of Water and Soil Conservation, Northwest Agriculture and Forestry University, Yangling, China

\* Correspondence: Huanjie Cai (huanjieci@yahoo.com); Zhongbo Su (z.su@utwente.nl)

155 **Abstract.** Root water uptake by plants is ~~an important component of the terrestrial water balance and a critical factor~~vital process that influences terrestrial energy, water ~~vapor~~, and carbon ~~exchange among exchanges~~. In the soil, vegetation, and atmosphere interfaces, root water uptake and solar radiation predominantly regulate the dynamics and health of vegetation growth, which can be remotely monitored by satellites, using the soil-plant relationship proxy – solar-induced chlorophyll fluorescence. However, most ~~of the~~ current ~~vegetation canopy~~ photosynthesis and fluorescence models do not account for root water uptake, which compromises their applications under water stressed conditions. To address this limitation, this study ~~integrates~~integrated photosynthesis, fluorescence emission, and transfer of energy, mass and momentum in the soil-plant-atmosphere continuum system, via a simplified ~~1D~~one-dimensional root growth model and a resistance scheme (~~from linking soil, through root zones, roots, leaves and plants, to atmosphere~~). The coupled model was evaluated with field ~~measurement~~measurements of a maize ~~canopy and grass canopies~~. The results indicated that the simulation of land surface fluxes was significantly improved ~~due to considering~~by the root water uptake coupled model, especially when ~~vegetation is experiencing severe~~the canopy experienced moderate water stress. This finding highlights the importance of enhanced soil heat and moisture transfer, as well as dynamic root ~~distribution~~growth, on simulating ecosystem functioning.

165 **Key words:** SCOPE model; STEMMUS model; Soil-Plant-Atmosphere Continuum (SPAC) system; Root Water Uptake (RWU); Root system growth

## 170 1. Introduction

Root water uptake (RWU) by plants is a critical process controlling water and energy exchanges between the land surface and the atmosphere, ~~and~~ as ~~well-as-a result~~ the plant growth. The representation of RWU is an essential component of eco-hydrological models that simulate terrestrial water, energy and carbon fluxes (Seneviratne et al., 2010; Wang and Smith, 2004). However, most of these models consider the above-ground processes in much greater detail than below-ground processes, and therefore, they have limited ability ~~to~~ represent the dynamic response of plant water uptake to water stress. A particular mechanism of importance for plants to mitigate water stress is the compensatory root water uptake (CRWU) which refers to the process by which water uptake from sparsely rooted but well-watered parts of the root zone compensates for stress in other parts (Jarvis, 2011). The failure to account for compensatory water uptake and the associated hydraulic lift from deep subsoil (Caldwell et al., ~~1998; Espeleta et al., 2004; Amenu and Kumar, 2007; Fu et al. 1998; Dawson, 1993~~2016) can lead to significant uncertainties in simulating the plant growth and corresponding eco-hydrological processes (~~Desborough, 1997; Lee et al., 2005; Seneviratne et al., 2010; Teuling et al., 2006; Zeng and Dai, 1998~~).

~~Furthermore, the macroscopic RWU model needs to calculate Hydraulic Redistribution (HR) (Caldwell et al., ~~Because 1998; Espeleta et al., 2004; Amenu and Kumar, 2007; Fu et al. 2016~~) (Table 1). Ideally, a RWU model is based on the soil plant-atmosphere continuum concept (SPAC-RWU), and considers the redistribution of soil water with compensatory water uptake as well as the flow of water from soil through the plant to the atmosphere.~~

the spatial (i.e., one dimensional vertical) pattern of RWU is determined by the spatial distribution of the root system, the knowledge of which is essential for predicting the spatial distribution of water contents and water fluxes in soils. The distribution of roots and their growth are in turn sensitive to various physical, chemical, and biological factors, as well as to soil hydraulic properties that influence the availability of water and oxygen for plants (Beaudoin et al., 2009). Many attempts have been made in the past to develop root growth models that account for the influence of various environmental factors such as temperature, aeration, soil water availability, and soil compaction. Existing root growth models ranged from complex, three-dimensional root architecture models (Bingham and Wu, 2011; Leitner et al., 2010; Wu et al., 2005) to much simpler root growth models that are implemented within more complex models such as EPIC (Williams et al., 1989) and DSSAT (Robertson et al., 1993). Most of these models reproduce the measured rooting depth very well, but the distribution of new growth root is based on empirical functions rather than biophysical processes (Camargo and Kemanian, 2016) (Table 1).

Modelling RWU ~~requires~~requires representation of above and below ground processes, which ~~is can be~~ realized ~~via~~considering the flow of water from soil through the plant to the atmosphere (i.e., Soil-Plant-Atmosphere Continuum, SPAC-RWU, model) (Guo, 1992). The SPAC-~~RWU~~ model represents a good compromise between simplicity (i.e., a small number of tuning parameters) and the ability to capture non-linear responses of RWU (and subsequently the ecosystem functioning) to drought events. Specifically, the SPAC-~~RWU~~ model calculates the CRWU term using the gradient between leaf water potential and

soil water potential of each soil layer. ~~The HR process is an extreme case of CRWU occurring when the transpiration is relatively small and the RWU terms in some soil layers are negative due to leaf water potential was higher than soil water potential.~~ The most important parameters in the SPAC-RWU model include the leaf water potential, stomatal resistance, and the root resistance. Different from other macroscopic models using the root distribution function, the SPAC-RWU model needs explicitly the root length density at each soil layer to calculate the root resistance for each soil layer (Deng et al. 2017). The most practical method for obtaining the root length density is using ~~the~~ root growth model.

~~To~~ On other hand, remote sensing of solar-induced chlorophyll fluorescence (SIF) has been deployed to understand and monitor the ecosystem functioning under drought stress, ~~the sub- using models for below and above ground are therefore needed to be coupled via the afore-mentioned resistance schemes, which control the flow of water from soil to root, root to plant and plant to atmosphere. Furthermore, the coupling should be realized also via the interface: one sub-model provides the boundary conditions for the other. The below ground process model simulates the Simultaneous Transfer of Energy, Momentum, and Mass in Unsaturated Soil (i.e., STEMMUS model), the running of which requires land surface energy fluxes and land surface temperature. On the other hand, the required surface boundary state and fluxes can be provided with the above ground process model, for example, the-vegetation photosynthesis model, and fluorescence (Zhang et al., 2020; Mohammed et al., 2019; Shan et al., 2019; Zhang et al., 2018).~~ SCOPE (Soil Canopy Observation, Photochemistry, and Energy Fluxes).

~~The SCOPE) is such a model-simulates, simulating canopy reflectance and fluorescence spectra in the observation directions, as well as photosynthesis, and evapotranspiration as functions of leaf optical properties, canopy structure, and weather variables (Van der Tol et al. 2009). SCOPE model provides a valuable means to study the link between vegetation appearance and ecosystem functioning, however, it does not consider the water budget in soil and vegetation. As such, there is no explicit parametrization of the effects of soil moisture variations on the photosynthetic or stomatal parameters. Consequently, soil moisture effects are only ‘visible’ in SCOPE model if the lack of soil moisture affects the optical or thermal appearance of the vegetation (i.e., during water stress period). The lack of such link between soil moisture availability and vegetation appearance compromises the capacity of SCOPE for predicting/simulating and predicting drought events- on vegetation functioning.~~

The change of vegetation optical appearance as a result of soil moisture variations can only explain partially the soil moisture effect on ecosystem functioning (Bayat et al., 2018), which leads to considerably biased estimations of ~~the gross primary productivity (GPP-(Gross Primary Productivity)) and evapotranspiration (ET-(Evapotranspiration))~~ in water limited conditions. This presents a challenge for using SCOPE ~~for to~~ ecosystems in arid and semi-arid areas, where water availability is the primary limiting factor for vegetation functioning. This challenge becomes even more relevant considering that soil moisture deficit or “ecological drought” is expected to increase in both frequency and severity at nearly all ecosystems around the world (Zhou et al., 2013). Bayat et al. (2019) incorporated the SPAC model into SCOPE to address water stress conditions at a grassland

site, but the coupled model neglected the dynamic ~~development of~~ root distribution at different soil layers and soil moisture serves only as a model input coming from measurements.

235 In this study, the modelling of above-ground ~~radiation, photosynthesis, fluorescence emission, and~~ energy fluxes in the vegetation layer (~~i.e., by~~ SCOPE) will be fully coupled with the soil heat and mass transfer ~~model by the~~ STEMMUS ~~model~~ (Simultaneous Transfer of Energy, Mass and Momentum in Unsaturated Soil-), ~~by considering RWU based on a root growth~~ model. The root growth model and the corresponding resistance scheme (from soil, through ~~root zones~~ roots and ~~plants~~ leaves, to atmosphere) will be integrated for the dynamic ~~modeling~~ modelling of water stress and root system, enabling the seamless modelling of soil-water-plant-energy ~~interactions, water and carbon exchanges, and thus directly linking the vegetation~~ dynamics (and its optical and thermal appearance) on-process-level to soil moisture variability. The next *section of methodology* describes the coupling scheme between SCOPE and STEMMUS models, followed by the *section of results* ~~verifying and discussion which verifies~~ the coupled SCOPE-STEMMUS-SCOPE model at a maize agroecosystem and a grassland ecosystem located in a semi-arid ~~region. The discussion session~~ regions and explores ~~and reveals~~ the dynamic responses of leaf water potential and root length density to water stress. The summary of this study and the further challenges  
240  
245 are addressed in the *section of conclusions*.

**Table 1. Comparison of LSMs and crop models in terms of sink term calculation of soil water balance.**

Model	Sink term calculation of soil water balance		Root water uptake process		
			Hydraulic redistribution (Richards and Caldwell, 1987)	Compensatory uptake (Jarvis, 2011)	Root distribution
LSMs	CLM5.0	Root length density of each soil layer and water stress is applied by the hydraulic conductance model (Lawrence et al. (2020))	Extreme case of CRWU	Following Darcy's Law for porous media flow equations	Empirical function depends on the plant functional type
	CLM4.5	Actual transpiration, root fraction of each soil layer and soil integral soil water availability (Fu et al., 2016)	The Ryel et al. (2002) function	Not considered	Empirical function
	CLM4.0	Actual transpiration, root fraction of each soil layer and soil integral soil water availability (Couvreur et al. 2012, Sulis et al., 2019)	HRWU scheme (RWU model based on hydraulic architecture)	HRWU scheme	Empirical function
	CLM3 & IBIS2	Actual transpiration, physical root distribution and the water availability in each layer (Zheng and Wang, 2007)	The Ryel et al. (2002) function	Dynamic root water uptake	Empirical function
	CoLM	Potential transpiration, root fraction in each layer and water stress factor (Zhu et al., 2017)	The Ryel et al. (2002) and the Amenu and Kumar (2007) function	Empirical approach with a compensatory factor	Empirical function
	JULES	Potential transpiration, root fraction of each soil layer and a weighted water stress in each layer (Eller et al., 2020)	Not considered	Not considered	Exponential distribution with depth
	Noah-MP	Based on the gradient in water potentials between root and soil, and root surface area (Niu et al., 2010)	Extreme case of CRWU	Following Darcy's law for porous media flow equations	Process-based 1D root surface area growth model
	CABLE	Based on the gradient in water potentials between the leaf, stem, and the weighted average of the soil (De Kauwe et al., 2020)	Extreme case of CRWU	Following Darcy's law for porous media flow equations	Empirical function
Crop Models	APSIM	Potential transpiration and water supply factor, but neglect root distribution (Keating et al., 2003)	Not considered	Not considered	Empirical function Linear decrease in soils with
	CropSyst	Difference in water potential between the soil and the leaf, and a total soil–root–shoot conductance (Stöckle et al., 2003)	Not considered	Considered by the leaf and soil water potential	No limitations to root exploration
	DSSAT	Water uptake per unit of root length is computed as an exponential function, and the actual RWU is the minimum of potential transpiration and the maximum capacity of root water uptake (Jones et al., 2003)	Not considered	Water uptake per unit of root length as a function of soil moisture	Using an empirical function
	EPIC	EPIC assumes that water is used preferentially from the top layers, and the potential water supply rate decreases exponentially downward (Williams et al., 2014)	Not considered	Not considered	Not considered
	SWAP	Based on the potential transpiration, root fraction and an empiric stress factor relationship (van Dam, 2000)	Not considered	Based on soil water potential	Function of relative rooting depth
	WOFOST	The simplest one, it calculates water uptake as a function of the rooting depth and the water available in that rooting depth without regard to the soil water distribution with depth (Supit et al., 1994)	Not considered	Not considered	Empirical function
	SPACSYS	According to empirical root length density distribution in a soil layer, potential transpiration and soil moisture (Wu et al., 2005)	Not considered	Not considered	1D (empirical function) or 3D root system (process based)
	STICS	Based on the potential transpiration, root fraction, and soil water distribution, but not process based (Beaudoin et al., 2009)	Not considered	Not considered	1D root length density profile

## 95 2. Methodology and Data

### 2.1. SCOPE and SCOPE\_SM Models

SCOPE is a radiative transfer and energy balance model (Van der Tol et al. 2009). It simulates the transfer of optical, thermal, and fluorescent radiation ~~of~~in the vegetation canopy and computes *ET* by using an energy balance routine. SCOPE includes a radiative transfer module for incident solar and sky radiation to calculate the top of canopy outgoing radiation spectrum, net radiation and absorbed photosynthetically active radiation (*aPAR*), a radiative transfer module for thermal radiation ~~generated~~internally emitted by soil and vegetation to calculate the top of canopy outgoing thermal radiation and net radiation, an energy balance module for latent heat, sensible heat and soil heat flux, and a radiative module for chlorophyll fluorescence to calculate the top of canopy radiance spectrum of fluorescence ~~at leaf level~~.

Compared to other radiative transfer models which simplify the radiative transfer processes based on Beer's law, SCOPE has well-developed radiative transfer modules which consider the various leaf orientation and ~~the~~ multiple scattering. SCOPE can provide detailed information about net radiation of every leaf within the canopy. Furthermore, SCOPE ~~is based on~~incorporates an energy balance ~~and it can simulate~~model which predicts not only the temperature of leaf but also the temperature of soil surface temperature ~~which is~~(i.e., a vital boundary condition needed by STEMMUS-). In ~~addition~~the original SCOPE, soil is treated in a very simple way with several empirical functions describing the ground heat storage. Later, Bayat et al. (2019) ~~developed SCOPE\_SM, which was based on~~extended the SCOPE ~~but considering~~model by including the ~~effect of~~ soil moisture ~~(as model inputs). Therefore,~~effects on the vegetation canopy, which results in the SCOPE\_SM model. This model takes soil moisture as input and predicts the effects on several processes of vegetation canopy by using the SPAC concept. Appendix A.1 lists the main equations of calculating water stress factor within SCOPE (Bayat et al. 2019), and the detailed formulation of SCOPE is referred to Van der Tol et al. (2009).

SCOPE\_SM provides the basic framework to couple SCOPE with ~~STEMMUS, however~~a soil process model. However, both SCOPE and SCOPE\_SM ignored the soil heat and mass transfer processes and the dynamics of root growth. This can be overcome by introducing the STEMMUS model. Appendix A.1 lists the main equations of calculating water stress factor within SCOPE (Bayat et al. 2019), the detailed formulation of SCOPE is referred to Van der Tol et al. (2009).

### 2.2. STEMMUS Model

STEMMUS model is a two-phase mass and heat transfer model with explicit consideration of the coupled liquid, vapor, dry air and heat transfer in unsaturated soil (Zeng et al. 2011a,b; Zeng and Su, 2013; Yu et al. 2018). STEMMUS provides a comprehensive description of water and heat transfer in the unsaturated soil, which can compensate what is currently neglected in SCOPE. The boundary condition needed by STEMMUS includes surface soil temperature, which is the output of SCOPE. In addition, STEMMUS already contained an empirical equation to calculate root water uptake and a simplified root growth

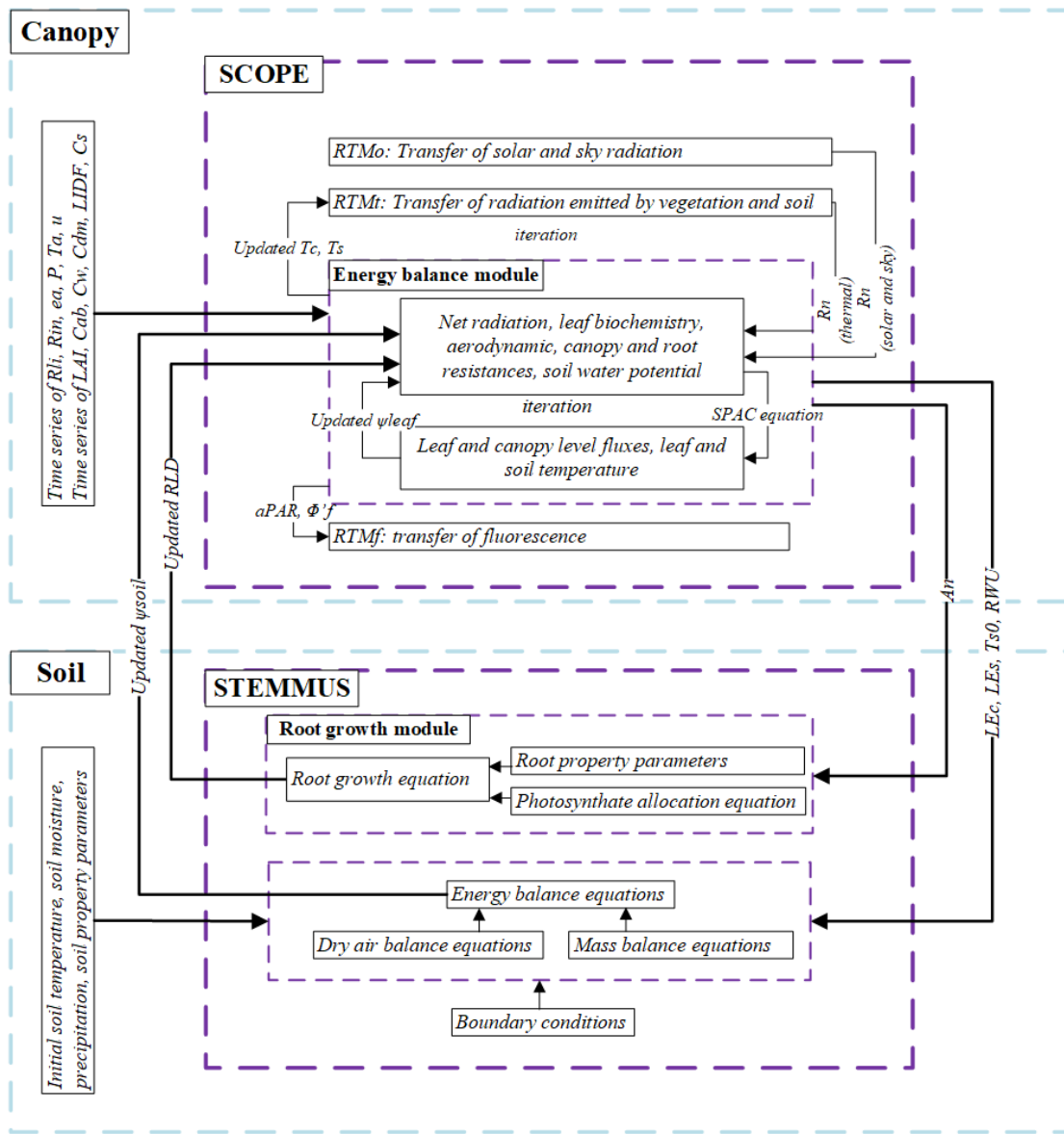
125 module to calculate root fraction profile. As such, STEMMUS has an ideal model structure to be coupled with SCOPE. The  
main governing equations of STEMMUS are listed in Appendix A.2.

### 2.3 Dynamic Root Growth and Root Water Uptake

130 To obtain the root resistance of each soil layer, we incorporated a root growth module to simulate the root length density profile  
(see Appendix A.3). The simulation of root growth refers to the root growth module in the INRA STICS crop growth model  
(Beaudoin et al., 2009), which includes the calculations of root front growth and root length growth. The root front growth is  
a function of temperature, with the depth of the root front beginning at the sowing depth for sown crops and at an initial value  
of transplanted crops or perennial crops (Beaudoin et al., 2009). The root length growth is calculated in each soil layer,  
considering the net assimilation rate and the allocation fraction of net assimilation ~~onto~~ root, which is ~~subsequently~~in turn a  
function of ~~LAI~~(leaf area index (LAI) and root zone water content (Krinner et al. 2005). The root length density profile is then  
135 used to calculate the root resistance to water flow radially across the roots, soil hydraulic resistance, and plant axial resistance  
to flow from the soil to the leaves (see Appendix ~~A4~~A.4).

### 2.4 ~~SCOPE-STEMMUS-SCOPE~~ Coupling

The coupling starts with an initial soil moisture ( $SM$ ) profile simulated by STEMMUS, which enables the calculation of the  
water stress factor, as a reduction factor of the maximum carboxylation rate ( $V_{cmax}$ ), SCOPE is then used to calculate net  
140 photosynthesis ( $A_n$ ) or gross primary productivity ( $GPP$ ), soil respiration ( ~~$R_e$~~  $R_s$ ), energy fluxes ( $R_n$ ,  $LE$ ,  $H$  and  $G$ ), transpiration  
( $T$ ), which is passed to STEMMUS as the root water uptake (RWU). Then, the ~~net ecosystem exchange ( $NEE$ )~~gross primary  
production ( $GPP$ ) can be calculated based on  $A_n$  ~~and  $R_e$~~ . Surface soil moisture is also used in calculating soil surface resistance  
and then calculating soil evaporation ( $E$ ). Furthermore, SCOPE can calculate soil surface temperature ( $T_{so}$ ) based on energy  
balance, which was subsequently used as the top boundary condition of STEMMUS. Based on RWU, STEMMUS calculates  
145 the soil moisture in each layer at the end of the time step, and the new soil moisture profile will be the soil moisture at the  
beginning of next time step, which is repeated as such till the end of simulation period. The time-step of ~~SCOPE-STEMMUS-~~  
SCOPE is flexible and the time step used in this study was half hour. Figure 1 shows the coupling scheme of STEMMUS and  
SCOPE, and Table B.1 shows all the parameter values used in this study.



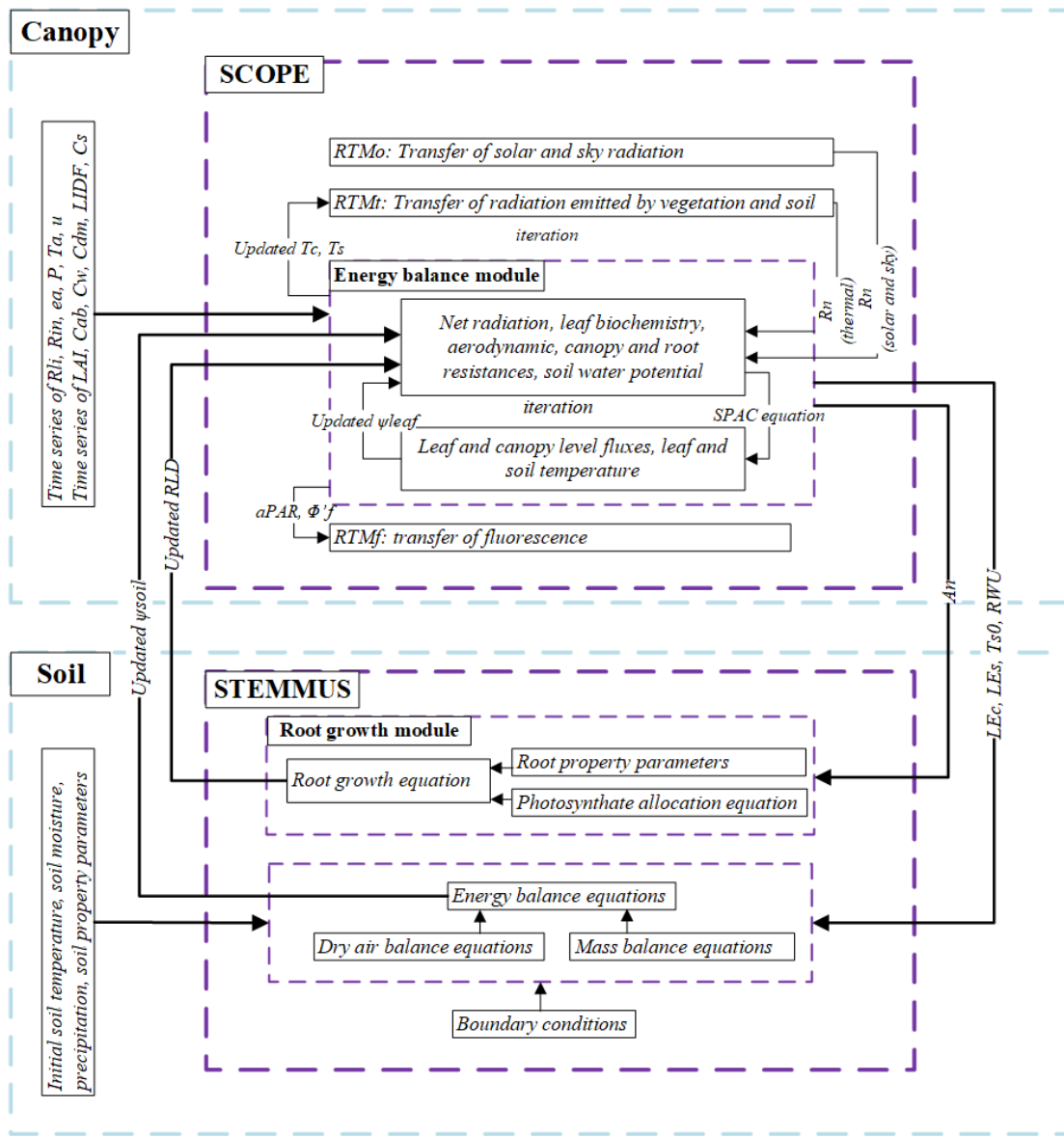


Figure 1. The coupling scheme of **SCOPE-STEMMUS** (Yu et al. (2018), Van der Tol et al. (2009))-SCOPE. The explanations of the symbols were the same as in Table B.1.

## 2.5. Evapotranspiration partitioning

Most studies in partitioning evapotranspiration ( $ET$ ) use sap flow and micro lysimeter data from in-situ measurements. In this study, we used a simple and practical method to separate evaporation ( $E$ ) and transpiration ( $T$ ) proposed by Zhou et al. (2016). Although the ~~behavior~~behaviour of plant stomata is influenced by environmental factors, the potential water use efficiency ( $uWUE_p$ ,  $\text{g C hPa}^{0.5}/\text{kg H}_2\text{O}$ ) at stomatal scale in the ecosystem with a homogeneous underlying surface is assumed to be nearly constant (Medlyn et al., 2011), and variations of actual  $uWUE$  ( $\text{g C hPa}^{0.5}/\text{kg H}_2\text{O}$ ) can be attributed to the soil evaporation (Zhou et al., 2016). Thus, the method can be used to estimate  $T$  and  $E$  with the quantities of  $ET$ ,  $uWUE$  and  $uWUE_p$ . Another assumption of this method is that the ecosystem  $T$  equal to  $ET$  at some growth stages, so  $uWUE_p$  can be estimated using the upper bound of the ratio of  $GPP\sqrt{VPD}$  to  $ET$  (here  ~~$GPP$~~  $VPD$  refers to ~~Gross Primary Productivity, and~~  $VPD$  to vapor pressure deficit) (Zhou et al., 2014; Zhou et al., 2016).

Zhou et al. (2016) used the 95<sup>th</sup> quantile regression between  $GPP\sqrt{VPD}$  and  $ET$  to estimate  $uWUE_p$ , and showed that the 95<sup>th</sup> quantile regression for  $uWUE_p$  at flux tower sites was consistent with the  $uWUE$  derived at the leaf scale for different ecosystems. In addition, the variability of seasonal and interannual  $uWUE_p$  was relatively small for a homogeneous canopy. Therefore, the calculations of  $uWUE_p$ ,  $uWUE$ , and  $T$  at the ecosystem scale were as follows:

$$uWUE_p = \frac{GPP\sqrt{VPD}}{T} \quad (1)$$

$$uWUE = \frac{GPP\sqrt{VPD}}{ET} \quad (2)$$

$$\frac{T}{ET} = \frac{uWUE}{uWUE_p} \quad (3)$$

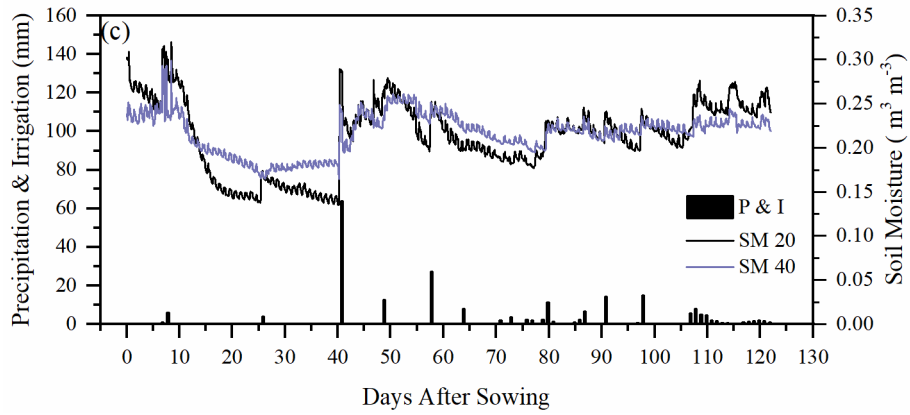
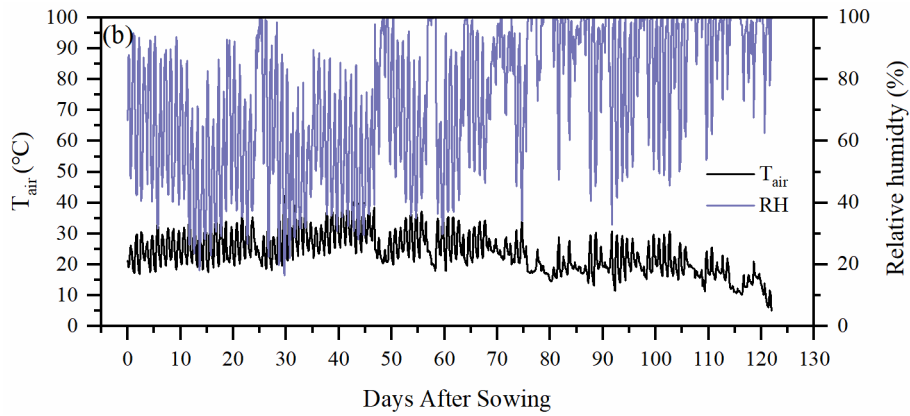
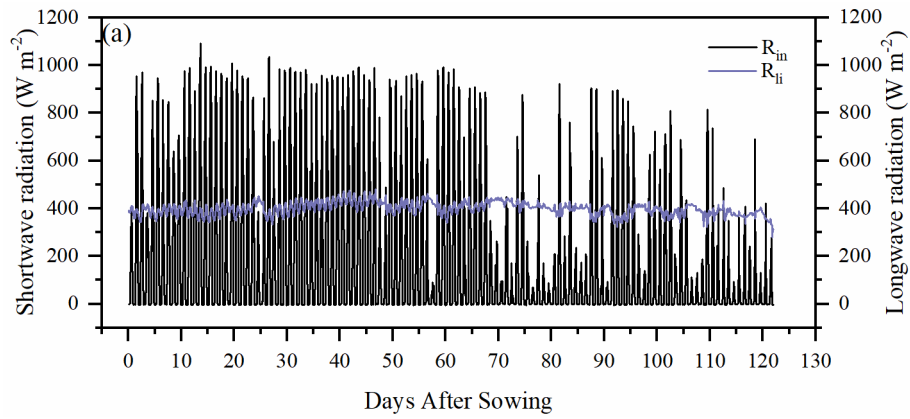
The calculation of  $VPD$  was based on air temperature and relative humidity data, and the method of gap-filling was the Marginal Distribution Sampling ( $MDS$ ) method proposed by Reichstein et al. (2005). To calculate  $GPP$ , the complete series of net ecosystem exchange ( $NEE$ ) was partitioned into gross primary production ( $GPP$ ) and respiration ( $Re$ ) using the method proposed by Reichstein et al. (2005). Finally,  $ET$  was calculated using the latent heat flux and air temperature. Based on  $GPP$ ,  $ET$  and  $VPD$  data,  $T$  can be calculated using the method proposed by Zhou et al. (2016).

~~Meanwhile, Zhou et al. (2016) discussed the uncertainty of this method, which was mainly caused by: (1) the uncertainty in the partitioning of  $GPP$  (less than 10%) and  $Re$  based on  $NEE$ , which would result in some uncertainty in  $uWUE$ ; (2) due to the seasonal variation of atmosphere  $\text{CO}_2$  concentration, the assumption of  $uWUE_p$  being constant would cause some uncertainty (less than 3%); (3) the assumption of  $T$  being equal to  $ET$  sometimes during the growing season would cause some uncertainty when vegetation is sparse.~~

## 180 **2.6. Field measurements**

### 2.6. Study site and data description

To evaluate the performance of SCOPE\_STEMMUS-SCOPE in ~~modeling~~ modelling ecohydrological processes, simulation was conducted to compare SCOPE\_STEMMUS-SCOPE with SCOPE, SCOPE\_SM, and STEMMUS using ~~the observation of fluxes (observations over a C4 cropland (Summer-maize: from 10 June 2017 to 10 October 2017)~~ at the Yangling station (34°17' N, 108°04' E, 521 m a.s.l.). ~~Figure 2 illustrates the variations of environmental factors during the maize growing season. As shown in the subfigures, the incoming shortwave radiation ranged from 0 to 1100 W m<sup>-2</sup>) and decreased significantly after Days After Sowing (hereafter as DAS) 67. In contrast, the incoming longwave radiation was relatively stable, which was about 400 W m<sup>-2</sup> during the maize season. The air temperature was relatively high a C3 grassland at initial stage and gradually decreased to 5 °C at the late stage. The soil moisture was maintained at a high level except during a drought episode from DAS 15 to 40, and the relative humidity (RH) at the late stage was higher than that at the early stage. Two irrigations were carried out on DAS 7 and DAS 41, and the volume of irrigation were 28mm and 64mm, respectively. The leaf area index (LAI) and canopy height (hc) were measured and the peak value was 4.39 m<sup>2</sup>·m<sup>-2</sup> and 1.95 m, respectively. Due to the lack of field measurement on root length and soil moisture profile of root zone, we used the simulated results of SCOPE\_STEMMUS as the input data of SCOPE\_SM to compare the performance of SCOPE\_SM with that of SCOPE\_STEMMUS. The Eddy Covariance (EC) system was installed on the Vaira Ranch (US-Var) Fluxnet site (38°25' N, 120°57' W, 129 m a height-adjustable tripod, The EC system included a three-dimensional sonic anemometer, an open path infrared gas analyser, and a data logger. The s.l.) (Annual grasses: from 1 June to 8 August 2004). The seasonal variation of precipitation, irrigation, and SM for these two sites were presented in Figure 2. And the main differences between these four models were presented in Table 2. In this study, the LAI data of Vaira Ranch (US-Var) Fluxnet site was from MODIS 8-daily LAI product instead of the field measured LAI used by Bayat et al. (2019). For the soil water content used by SCOPE\_SM, the averaged root zone soil moisture was used for Yangling station and the soil moisture at 10 cm depth was used for Vaira Ranch site. More detailed descriptions of the instruments these sites and data can refer to Wang et al. (2020(2019; 2020a) and Bayat et al. (2018; 2019).~~



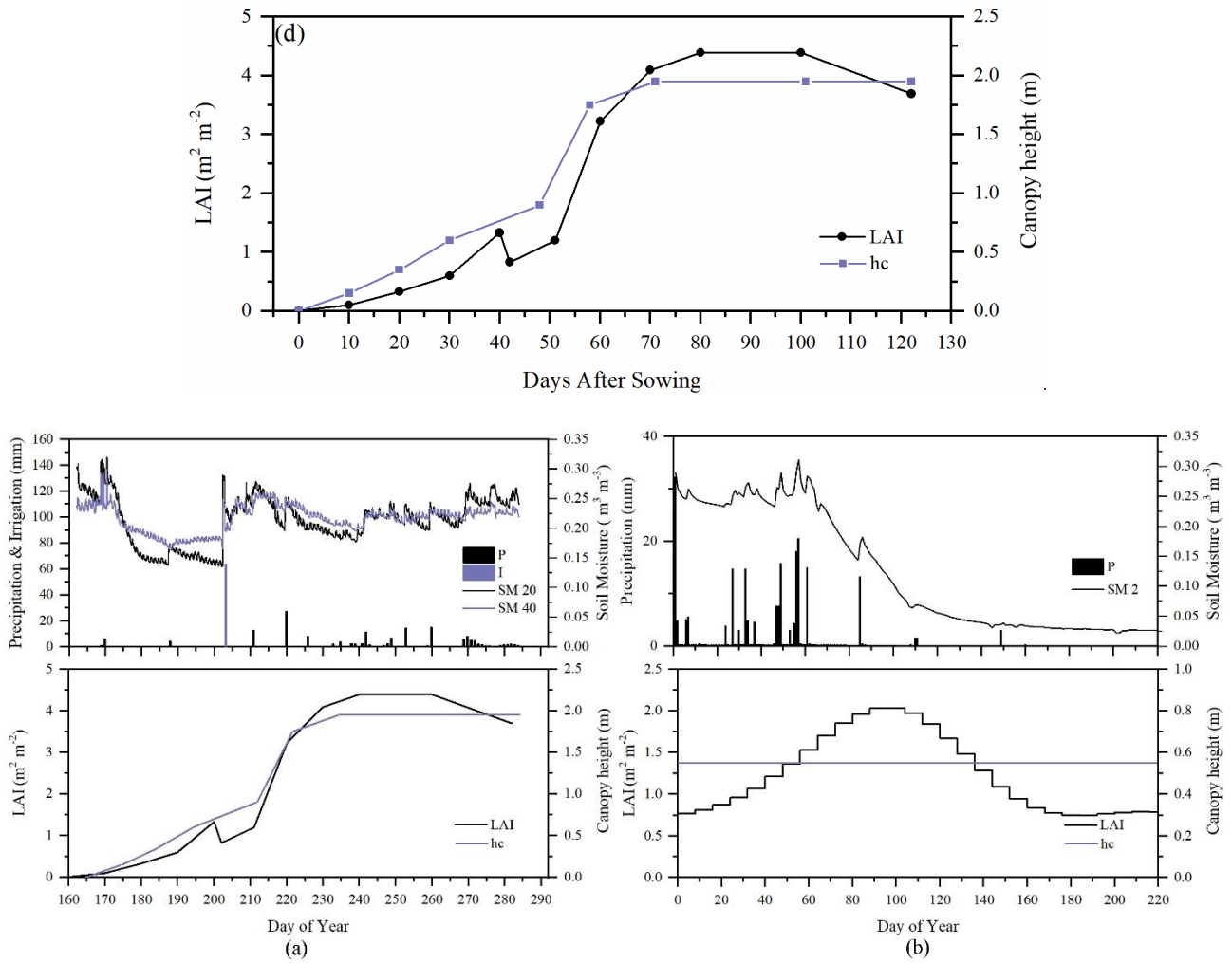


**Figure 2** Seasonal variation of environmental factors for maize growing season at Yangling, China. (a) incoming shortwave radiation ( $R_{in}$ ) and incoming longwave radiation ( $R_{li}$ ); (b) air temperature ( $T_{air}$ ) and relative humidity (RH); (c) volumetric soil water content at 20, and 40 cm depths (SM 20, and SM 40) and daily precipitation ( $P$ ), irrigation ( $P&I$ ); (d) leaf area, soil moisture at 2cm (SM 2), 20 cm (SM 20), 40 cm depth (SM 40), Leaf area index (LAI), and canopy height ( $h_c$ ); (a) Maize cropland at Yangling station; (b) Grassland at Vaira Ranch (US-Var) Fluxnet site.

**Table 2. Main differences among SCOPE, SCOPE\_SM, STEMMUS, and STEMMUS-SCOPE.**

	SCOPE	SCOPE_SM	STEMMUS	STEMMUS-SCOPE
Source	Van der Tol et al. (2009)	Bayat et al. (2019)	Zeng et al. (2013)	This study
Soil surface resistance calculation	Set $SM$ as constant or field measured surface $SM$	Field measured surface $SM$	Simulated surface $SM$ by itself	Simulated surface $SM$ by itself
$WSF$ calculation	Set $SM$ as constant	Field measured $SM$	Simulated $SM$ by itself	Simulated $SM$ by itself
$ET$ calculation	Process based (Analogy with Ohm's law)	Process based (Analogy with Ohm's law)	Penman–Monteith model or FAO dual crop coefficient method	Process based (Analogy with Ohm's law)
Photosynthesis	Farquhar and Collatz model	Farquhar and Collatz model	Absent	Farquhar and Collatz model
Radiation transfer	SAIL4 model	SAIL4 model	Based on Beer's law	SAIL4 model
$T_sO$	Simulated by itself	Simulated by itself	Field measured	Simulated by itself
$RWU$ calculation	Absent	Absent	Based on potential $T$ , root fraction, and soil moisture profile	Based on leaf and soil water potential
Root growth	Absent	Absent	Empirical model	Process-based model

## 2.7. Performance Metrics

215 The metrics used to evaluate the performance of coupled SCOPE\_STEMMUS-SCOPE model include: (1) Root Mean Squared Error ( $RMSE$ ); (2) coefficient of determination ( $R^2$ ); and (3) the index of agreement ( $d$ ). They are calculated as:

$$RMSE = \sqrt{\frac{1}{n} \sum_{i=1}^n (P_i - O_i)^2} \quad (4)$$

$$R^2 = \frac{[\sum_{i=1}^n (P_i - \bar{P})(O_i - \bar{O})]^2}{|\bar{O}| \sum_{i=1}^n (P_i - \bar{P})^2 \sum_{i=1}^n (O_i - \bar{O})^2} \quad (5)$$

$$220 \quad d = 1 - \frac{\sum_{i=1}^n (P_i - O_i)^2}{\sum_{i=1}^n (|P_i - \bar{O}| + |O_i - \bar{O}|)^2} \quad (6)$$

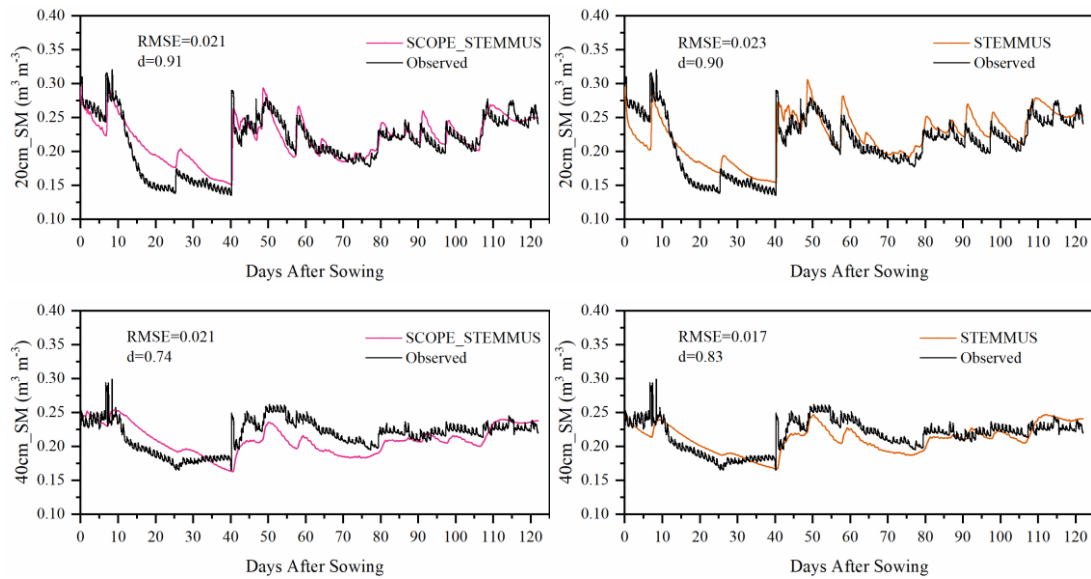
where  $P_i$  is the  $i$ th predicted value,  $O_i$  is the  $i$ th observed value,  $\bar{O}$  is the average of observed values, and  $n$  is the number of samples.

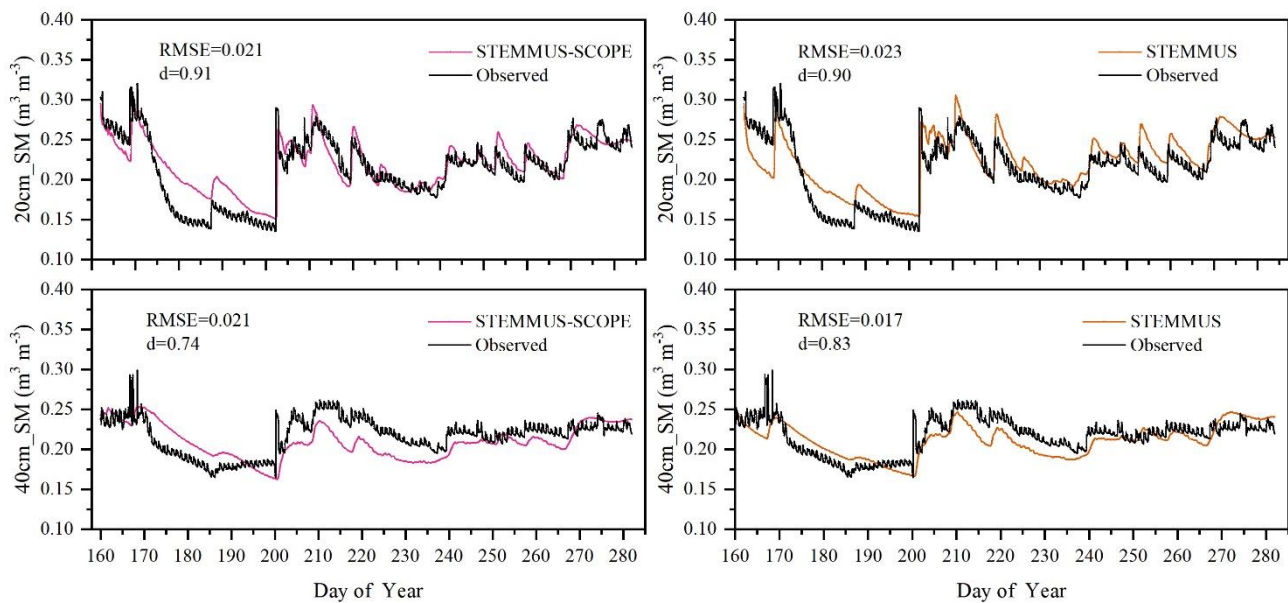
## 3. Results and discussion

### 3.1. Soil moisture modelingmodelling

225 ComparisonAs the soil moisture profile was not available in US-Var site, the comparisons of simulated soil moisture ( $SM$ ) at Yangling station using STEMMUS and SCOPE\_STEMMUS-SCOPE and observed ones isare presented in Figure 3. The simulated soil moisture at 20 cm depth agreed with the observed values in terms of seasonal pattern. Although slight overestimation occurred at initial and late stages, the dynamics in soil moisture resulted from precipitation or irrigation were

well captured. Per the nature of the two models, the coupling of SCOPE with STEMMUS is not expected to improve the simulation of soil moisture. However, compared to SCOPE\_SM, which used soil moisture measurements as inputs, the coupled SCOPE\_STEMMUS-SCOPE improves the simulation of soil moisture dynamics as measured. The deviation between the model simulations and the measurements can be attributed to the following two potential reasons. First, the field observation has errors to a certain extent and the soil moisture sensors may be not well calibrated. Second, in this simulation, we assumed that the soil texture was homogeneous in the vertical directionprofile, whereas the soil properties (e.g. soil bulk density and saturated hydraulic conductivity) may vary with depth in reality, and at different growth stages due to field management practices. For example, the soil bulk density at 40 cm was much higher than that at 20 cm due to the mechanical tillage, especially in the early stage.





240

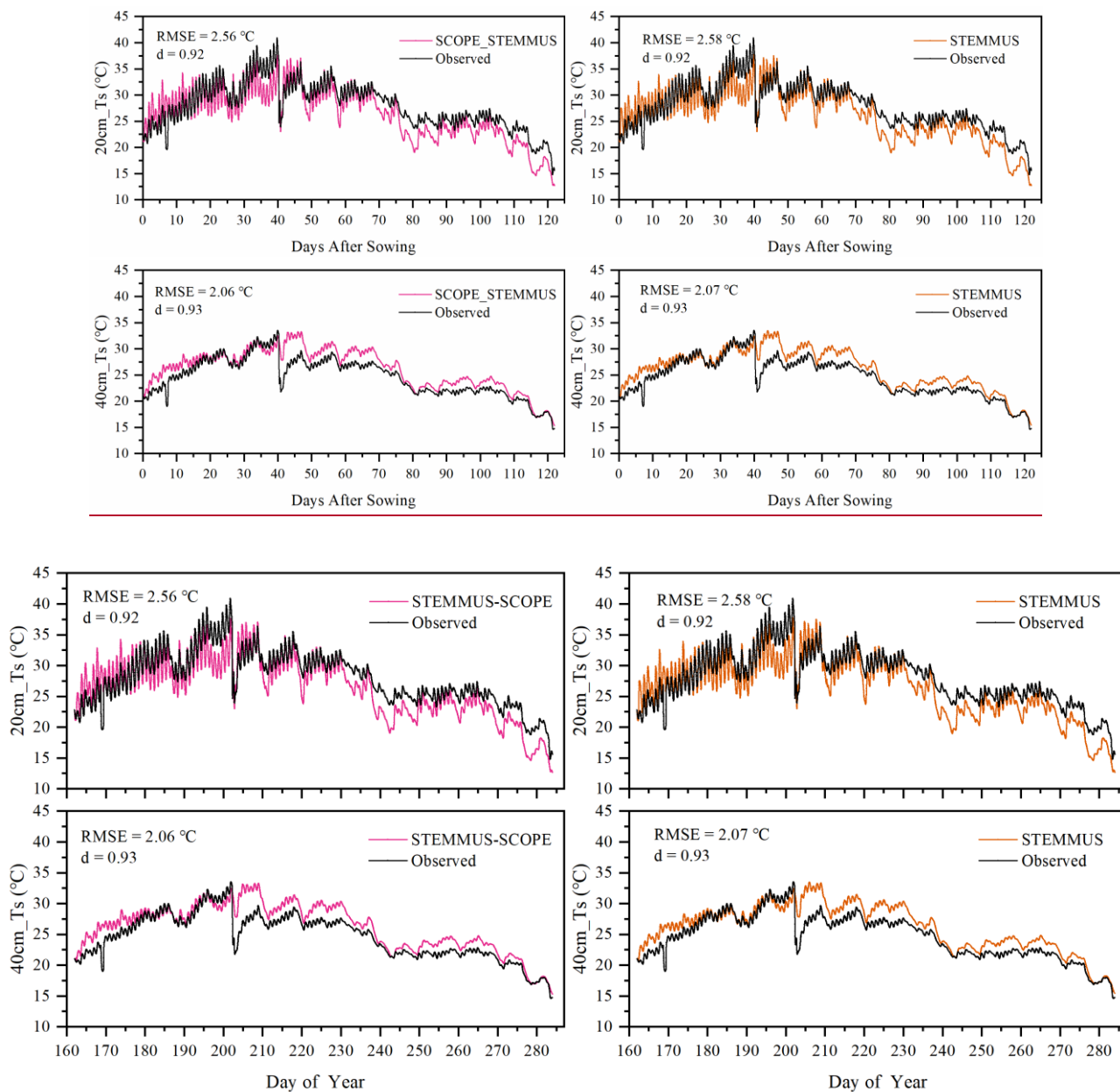
**Figure 3 Comparison of modeled and observed and modeled soil moisture at 20 cm (20 cm\_SM) and 40 cm depth (40 cm\_SM) for the maize cropland at Yangling station.**

### 3.2. Soil temperature modeling/modelling

245 Similar to soil moisture, only simulated soil temperatures ( $T_s$ ) at Yangling site by STEMMUS and SCOPE-STEMMUS-SCOPE at 20 cm and 40 cm depth are shown in Figure 4. In general, both two models can capture the dynamie dynamics of soil temperature well. For the simulation of 20 cm-temperature, for STEMMUS and SCOPE-STEMMUS, at 20 cm, the RMSE value was 2.56 °C and 2.58 °C, respectively; and d value was 0.92 and 0.92, for STEMMUS and STEMMUS-SCOPE respectively. For the simulation of 40cm-temperature, at 40cm, the RMSE value was 2.06 °C and 2.07 °C, respectively; and d value was 0.93 and 0.93, respectively. These results indicate that both models can simulate well soil temperature. However, there also exist some differences between simulation and observation. The largest difference occurred in DAS 40DOY 202, when the field was irrigated with the flooding irrigation method. This irrigation activity may lead to the boundary condition errors (i.e., for soil surface temperature), which cannot be estimated well enough (e.g., there is no monitoring of water temperature from the irrigation). Meanwhile, the measurement may also have some errors in this period. The fact for the observed soil temperature at 20 cm and 40 cm to decrease/decreasing to almost the same level at the same time indicates a potential pathway for preferential flow in the field (see precipitation/irrigation at DAS 40DOY 202 in Figure 2), and the sensors captured this phenomenon. Nevertheless, the model captures the soil temperature dynamics.

250

255

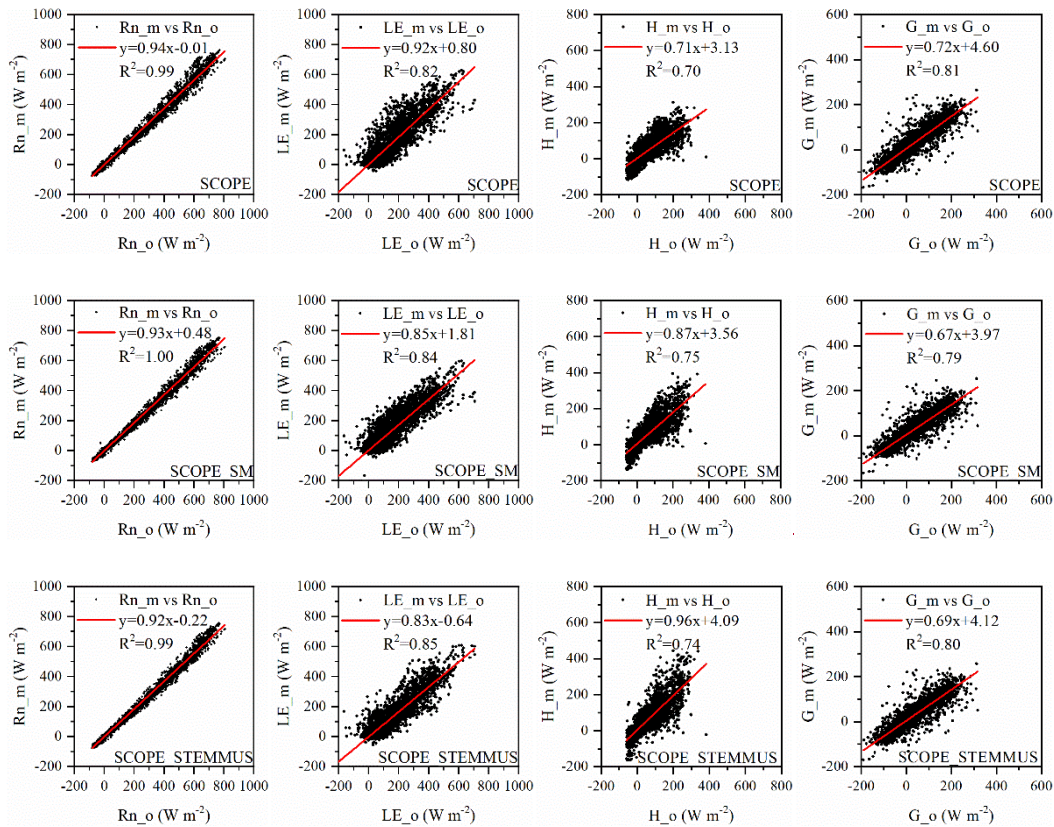


260 **Figure 4 Comparison of observed and modeled soil temperature at 20 cm (20 cm\_Ts) and 40 cm depth (40 cm\_Ts) for the maize cropland at Yangling station.**

### 3.3. Energy balance ~~modeling~~modelling

A comparison of the ~~modeled and~~ modeled and ~~observed and modeled~~ half-hourly net radiation ( $Rn$ ), sensible heat flux ( $H$ ), latent heat flux ( $LE$ ), and soil heat flux ( $G$ ) using ~~original-SCOPE~~, SCOPE\_SM, and ~~SCOPE\_STEMMUS-were-SCOPE~~ are presented in

265 Figure 5: (STEMMUS uses  $R_n$  as driving data and therefore is not included in the comparison). For net radiation and soil heat flux, the simulations of all three models show good agreements with observations. For net radiation, and the coefficient of determination ( $R^2$ ) for SCOPE, SCOPE\_SM and SCOPE\_STEMMUS were SCOPE was 0.99, 1.00, and 0.99, respectively. For soil heat flux, the  $R^2$  for SCOPE, SCOPE\_SM and SCOPE\_STEMMUS were SCOPE was 0.81, 0.79, and 0.80, respectively. For latent heat flux, SCOPE\_STEMMUS SCOPE has a better performance than SCOPE and SCOPE\_SM, and the  $R^2$  for SCOPE, SCOPE\_SM and SCOPE\_STEMMUS were SCOPE was 0.82, 0.79, and 0.85, respectively. Furthermore, SCOPE\_STEMMUS SCOPE and SCOPE\_SM have a similar performance in the simulation of sensible heat flux, which were better than the performance of SCOPE, and the  $R^2$  for SCOPE, SCOPE\_SM and SCOPE\_STEMMUS were SCOPE was 0.70, 0.75, and 0.74, respectively.



275

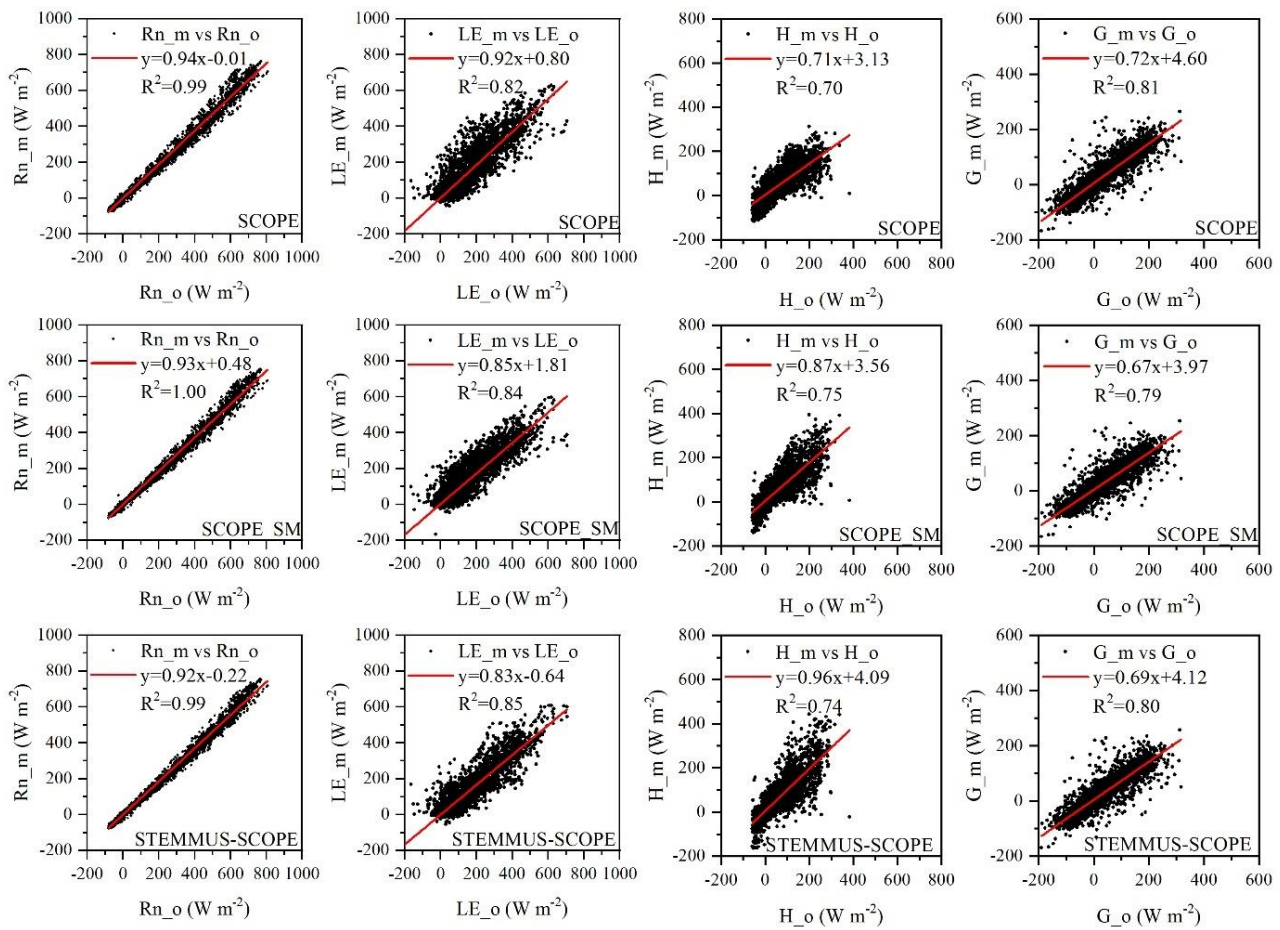


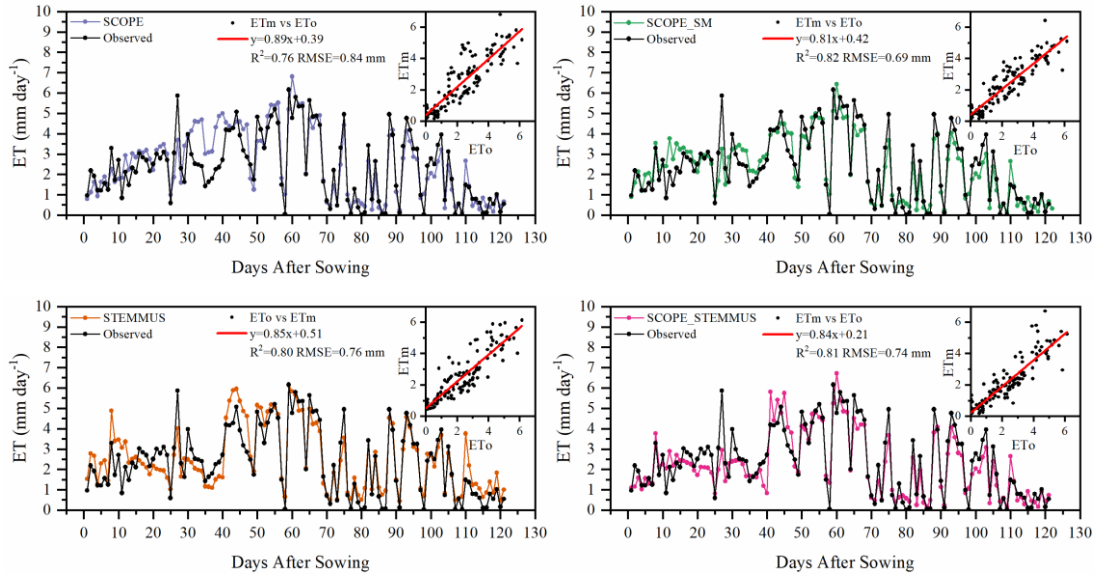
Figure 5 Comparison of modelled and observed and modeled half-hourly net radiation (Rn), latent heat (LE), sensible heat (H) and soil heat flux (G) by SCOPE, SCOPE\_SM and SCOPE\_STEMMUS-SCOPE at Yangling station. Subscripts 'm' and 'o' in each plot indicate indicates modeled and observed quantities, respectively. The regression line is indicated in red color with the corresponding regression equation and the  $R^2$ .

### 3.4. Daily ET, T and E modeling modelling

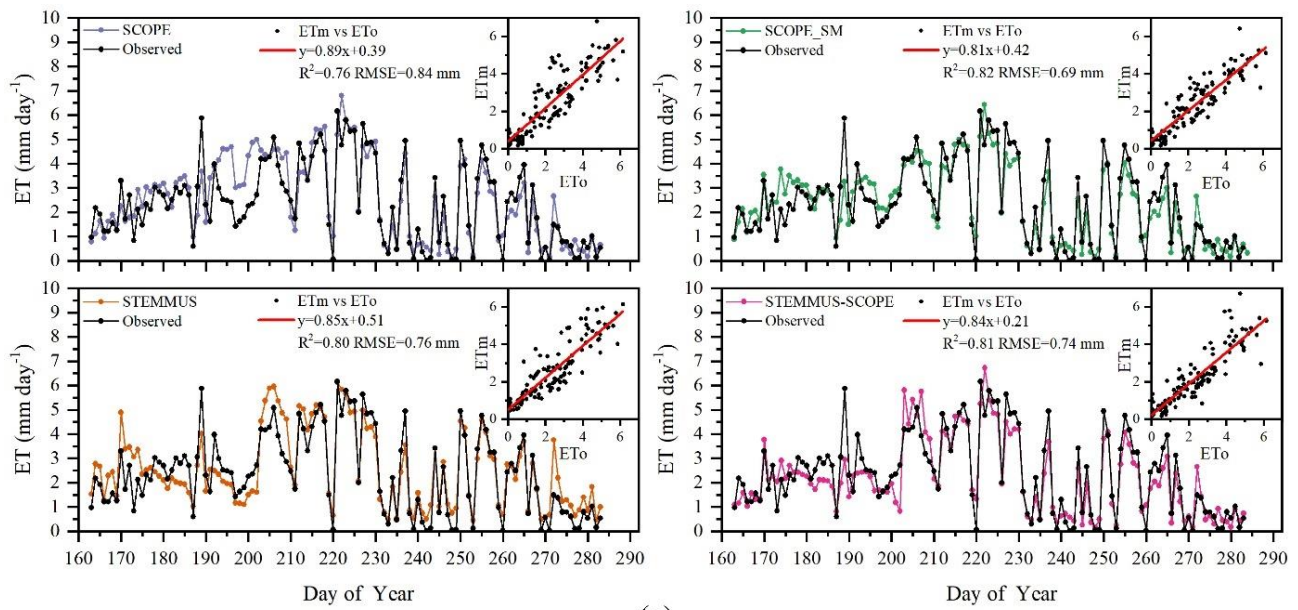
Simulated daily evapotranspiration (ET) results by SCOPE, SCOPE\_SM, STEMMUS and SCOPE\_STEMMUS-SCOPE are presented in Figure 6. As shown in For the subfigures Yangling station, the  $R^2$  by SCOPE, SCOPE\_SM, STEMMUS and SCOPE\_STEMMUS-SCOPE were SCOPE was 0.76, 0.82, 0.80 and 0.81, respectively, and the RMSE of these four models were was 0.84, 0.69, 0.76, and 0.74 mm day<sup>-1</sup>, respectively. For the US-Var station, the  $R^2$  by SCOPE, SCOPE\_SM, STEMMUS and STEMMUS-SCOPE was 0.10, 0.66, 0.84 and 0.89 and the RMSE was 1.83, 0.63, 0.40, and 0.34 mm day<sup>-1</sup>, respectively. For the ET simulation by SCOPE, there were large differences between simulations and observations when the vegetation suffered water stress. For SCOPE\_SM, STEMMUS and SCOPE\_STEMMUS-SCOPE, because of taking into account including the dynamic variation dynamics of soil moisture, the simulated ET were closer to observations when the crop vegetation

295

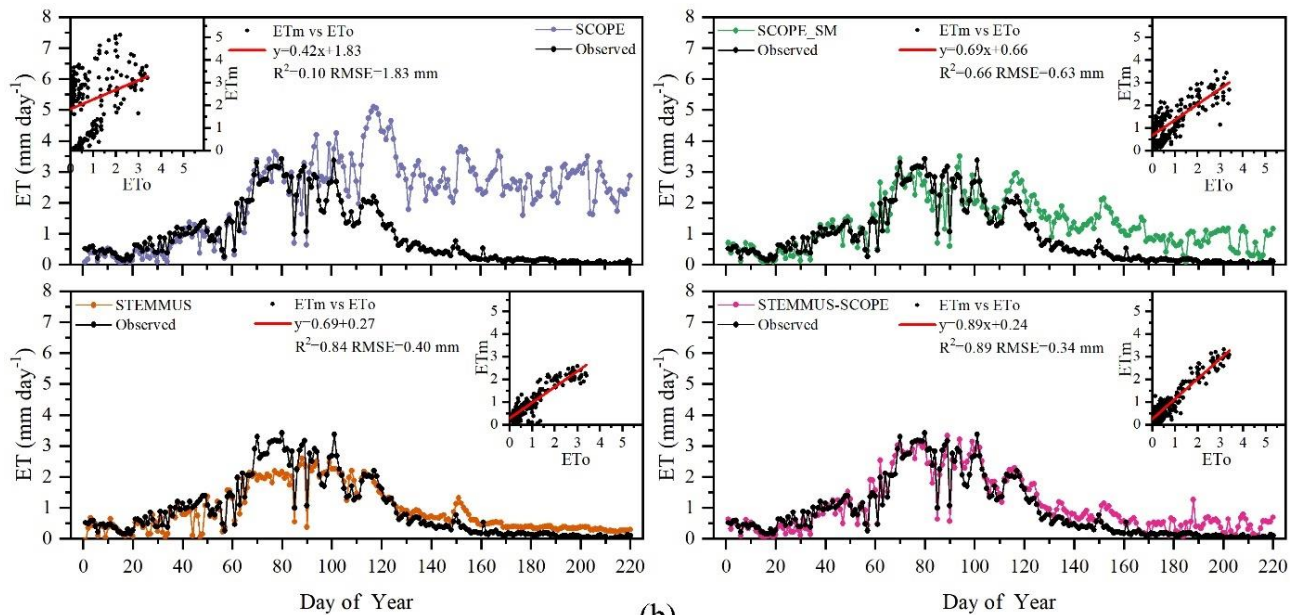
experienced water stress. It indicates that SCOPE\_STEMMUS\_SCOPE, STEMMUS and SCOPE\_SM can predict ET with a relatively higher accuracy, especially when the maize was under severe water stress (DAS 30 DOY 193 to 40), 202 at Yangling station and SCOPE\_DOY 90 to 220 at US-Var site), and STEMMUS\_SCOPE and SCOPE\_SM performed similarly well. It is noteworthy that although STEMMUS has considered the effect of soil moisture on ET, the accuracy of STEMMUS was lower than the coupled model (see DAS 40 and DAS 110 in Figure 6). The possible reason is the better representation of transpiration in SCOPE model (see Figure 7), which separates the canopy into 60 layers, while STEMMUS only treats the canopy as one layer. Besides, the coupled model performed better at grassland than at maize cropland. The reason is that the grassland simulation used the dynamic  $V_{cmax}$  data while the maize simulation used a constant  $V_{cmax}$  data.



300



(a)

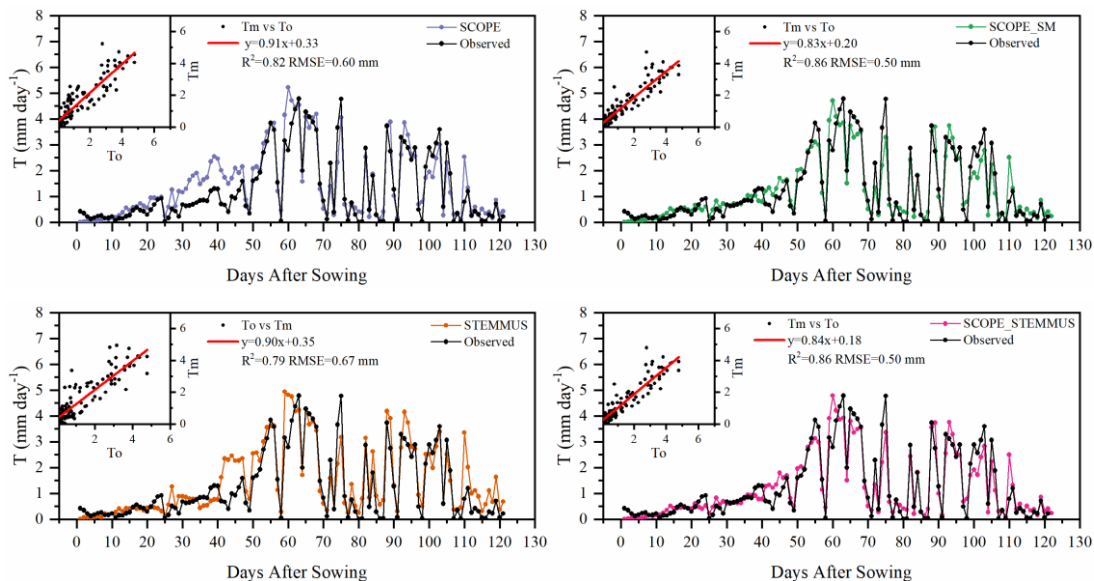


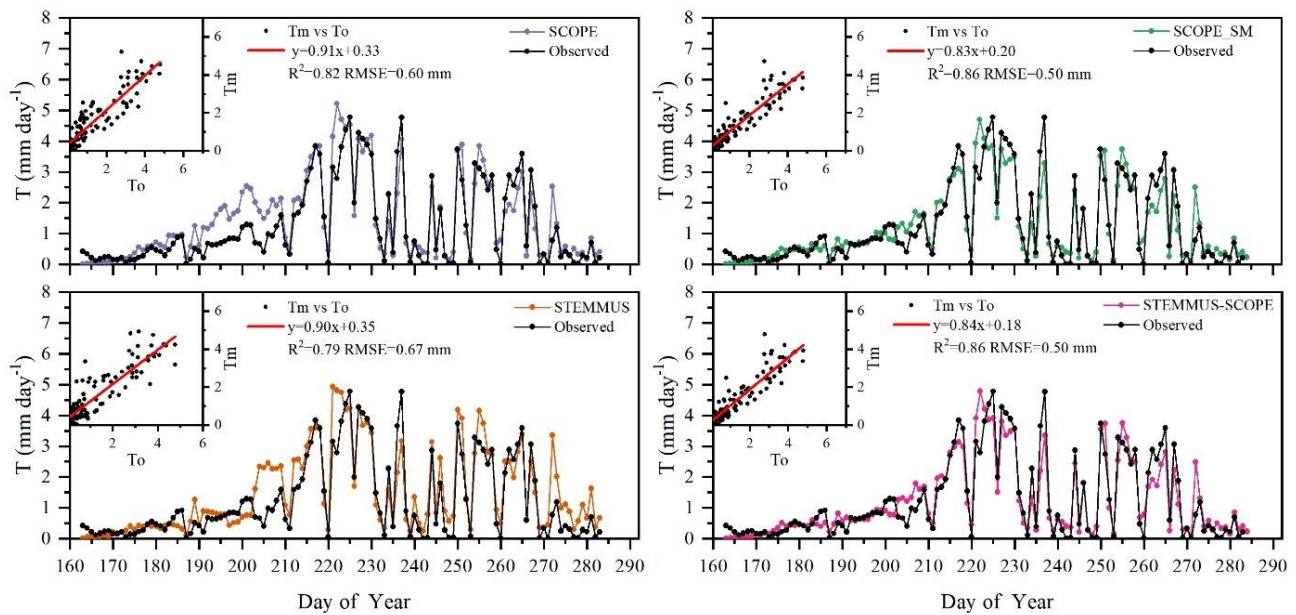
(b)

**Figure 6 Comparison of modeled and observed daily evapotranspiration (ET) (–): (a) Maize cropland at Yangling station; (b) Grassland at Vaira Ranch (US-Var) Fluxnet site. (ETm: modeled ET; ETo: observed ET; ETm: modeled ET).**

305 The modeled and observed daily plant transpiration at maize cropland are presented in Figure 7, and the modeled transpiration at grassland is presented in Figure 8. For Yangling station, the  $R^2$  value between simulated and observed transpiration were was

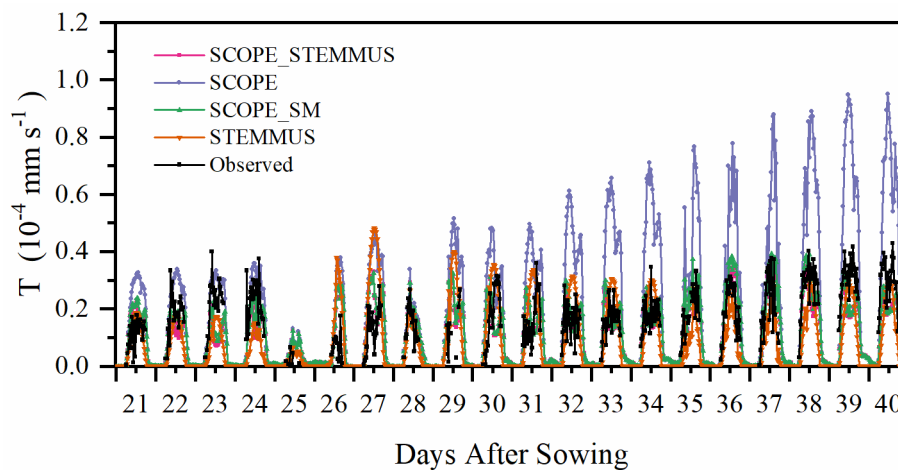
0.82, 0.86, 0.79, and 0.86, respectively, for SCOPE, SCOPE\_SM, STEMMUS and SCOPE\_STEMMUS, and the RMSE values were 0.60, 0.50, 0.67, and 0.50 mm day<sup>-1</sup>, for SCOPE, SCOPE\_SM, STEMMUS and SCOPE\_STEMMUS, respectively. Because of ignoring the effect of water stress on transpiration, SCOPE failed to simulate transpiration accurately when the vegetation experiencing water stress. As shown in the Figure 6(a), SCOPE overestimated transpiration for the maize cropland at Yangling station from DAS 20 DOY 183 to DAS 40 DOY 202 during the water stress period. Compared with SCOPE, SCOPE\_SM, STEMMUS and SCOPE\_STEMMUS-SCOPE can capture the reduction of transpiration during the dry period. The performances of SCOPE\_STEMMUS-SCOPE and SCOPE\_SM were also better than that of STEMMUS. The possible reason is the better simulation of the radiative transfer and energy balance at leaf level in the coupled SCOPE\_STEMMUS-SCOPE model (as also in SCOPE\_SM) and the more accurate root water uptake (compared to that in SCOPE\_SM). Nevertheless, SCOPE\_STEMMUS-SCOPE slightly underestimated transpiration when the plant is undergoing severe water stress and slightly overestimated it after the crop field was irrigated. This is mainly because the actual  $V_{cmax}$  was not only influenced by drought but also related to leaf nitrogen content (Xu and Baldocchi, 2003), which was not considered in this study the maize cropland simulation. Although the measured  $T$  at the grassland was not available, we compared modeled  $T$  by the four models (Figure 7). During the wet season (before DOY 85), the modeled  $T$  by SCOPE, SCOPE\_SM, and STEMMUS-SCOPE were similar and were higher than that by STEMMUS from DOY 64 to 82. During the dry season (after DOY 85), due to the simplified consideration of soil processes, the modeled  $T$  by SCOPE and SCOPE\_SM were both much higher than that by STEMMUS and STEMMUS-SCOPE. The reason for the better performance by the coupled model for the grassland (Figure 6(b)) is that it considers also the effect of leaf chlorophyll content ( $C_{ab}$ ) on  $V_{cmax}$ , in addition to more detailed consideration of water stress as discussed above for the maize cropland.

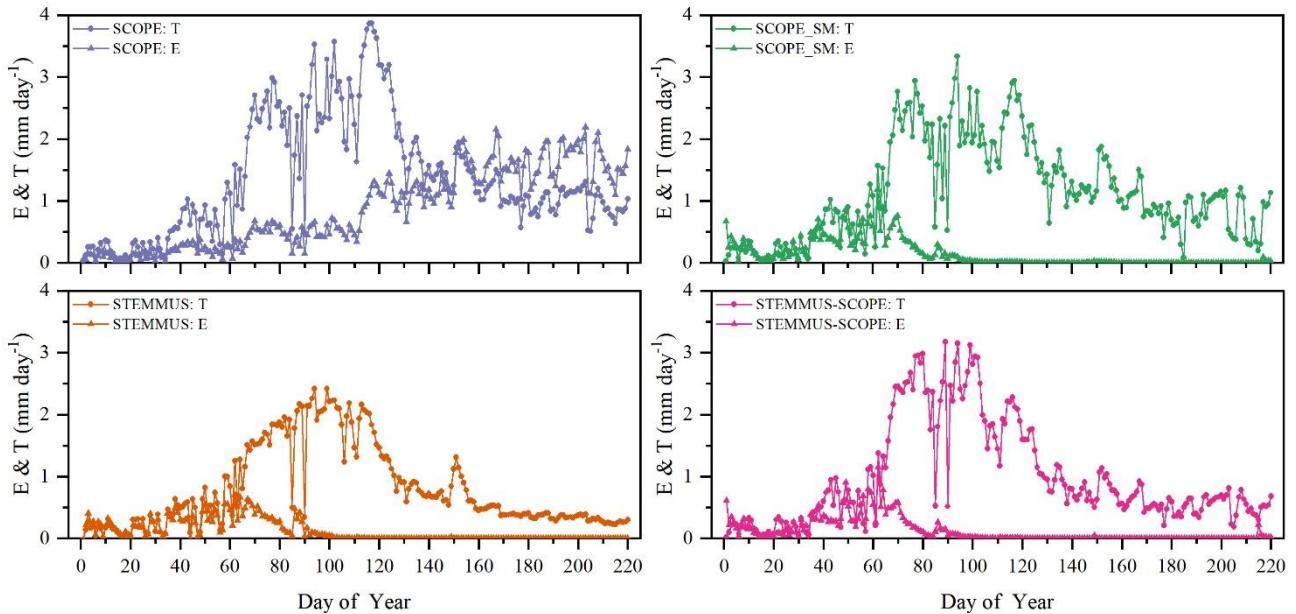




330 **Figure 7 Comparison of modeled and observed and modeled-daily plant transpiration (T) (for the maize cropland at Yangling station (Tm: modeled T; To: observed T; Tm: modeled T)).**

335 ~~Figure 8 shows the modeled and observed half hourly canopy transpiration. The simulations by SCOPE\_STEMMUS and SCOPE\_SM are consistent with observation and both are much lower than that by SCOPE. The performances of SCOPE\_STEMMUS and SCOPE\_SM were consistent with that of SCOPE in the early morning and late afternoon, when the photosynthesis is mainly limited by incident radiation rather than by water stress, intercellular CO<sub>2</sub>-concentration and V<sub>emax</sub>. In the midday, with increasing incident radiation, the photosynthesis was mainly limited by water stress and V<sub>emax</sub>, exactly when the simulations by SCOPE\_STEMMUS and SCOPE\_SM are much better than that by SCOPE.~~





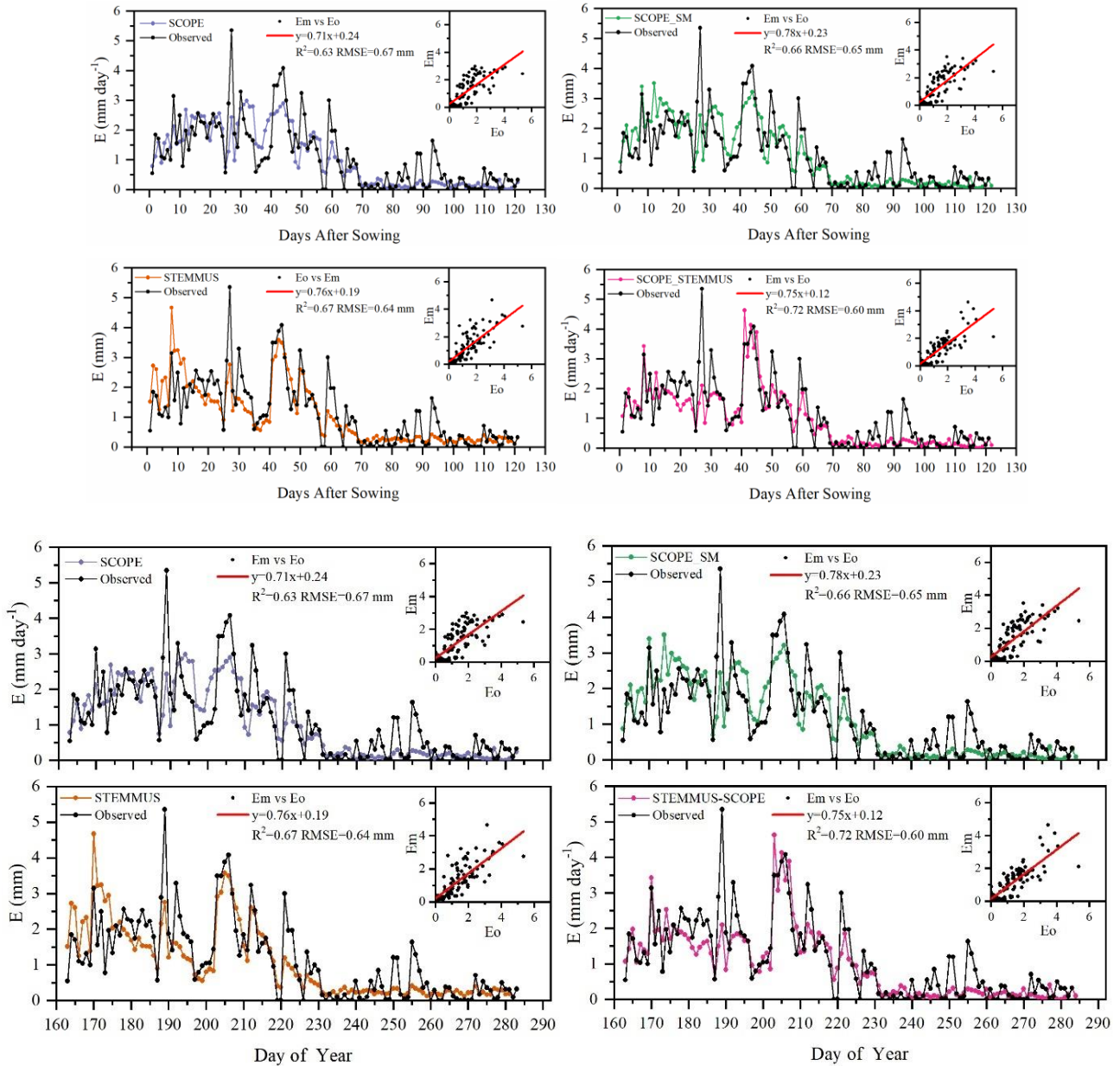
340 **Figure 8 Comparison of observed and modeled half-hourly/daily transpiration (T) and soil evaporation (E) for grassland at Vaira Ranch (US-Var) Fluxnet site (T: transpiration; E: soil evaporation).**

As shown in Figure 9 for soil evaporation at Yangling station, the simulation by SCOPE\_STEMMUS-SCOPE is closer to observation than those by other models. When using SCOPE to simulate soil evaporation, the soil moisture is set as constant (i.e.,  $0.25 \text{ m}^3 \text{ m}^{-3}$ ). Therefore, SCOPE generally underestimates soil evaporation when soil moisture is higher than 0.25 and overestimates soil evaporation-it when it is lower than 0.25. Due to the lack of measurement of soil surface moisture in this study, Here we use the average soil moisture at root zone simulated by SCOPE\_STEMMUS-SCOPE as the input data for SCOPE and SCOPE SM to calculate soil surface resistance and soil evaporation. Although STEMUSSTEMMUS can capture variation of soil evaporation reasonably well, it has higher *RMSE* value than SCOPE\_STEMMUS-SCOPE. This is probably attributed to the comprehensive consideration of radiation transfer in SCOPE, which is lacking in STEMMUS. Consequently, the simulation of soil net radiation ofby the coupled model was more accurate than that by STEMMUS alone. The *RMSE* value of SCOPE-by STEMMUS-SCOPE was  $0.60 \text{ mm day}^{-1}$ , which was lower than those ofby other three models (i.e. 0.67, 0.65, and  $0.64 \text{ mm day}^{-1}$  respectively). For SCOPE\_STEMMUS-SCOPE, the major differences between simulations and observations occurred in rainy days, or irrigation days (cf. Figure 2(a)), which may be caused by errors of the estimated soil surface resistance estimation during these periods or the uncertainty of ET partitioning method. The uncertainty of ET partitioning method (Zhou et al., 2016) was mainly caused by: (1) the uncertainty in the partitioning of *GPP* (less than 10%) and *Re* based on *NEE*, which would result in some uncertainty in *uWUE*; (2) due to the seasonal variation of atmosphere  $\text{CO}_2$  concentration, the assumption of  $uWUE_p$  being constant would cause some uncertainty (less than 3%); (3) the assumption of

350

355

*T* being equal to *ET* sometimes during the growing season would cause some uncertainty when vegetation is sparse. Because the observed *E* at US-Var site was not available, a comparison of only modeled *E* was shown in Figure 8, in which SCOPE modeled unrealistic *E* during the dry season, while the modeled *E* by SCOPE SM, STEMMUS, and STEMMUS-SCOPE were consistent due to use the simulated surface *SM* as the input for soil evaporation calculation.



365 **Figure 9 Comparison of modeled and observed ~~and modeled~~ daily soil evaporation (E) (at Yangling station (Em: modeled E; Eo: observed E; ~~Em: modeled E~~).**

### 3.5. Daily ~~NEE modeling~~GPP modelling

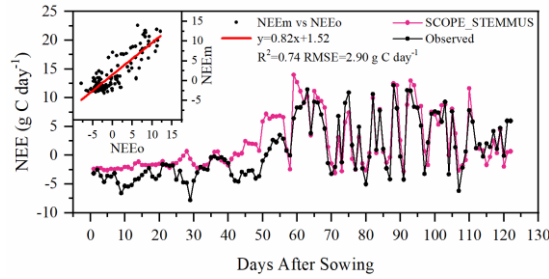
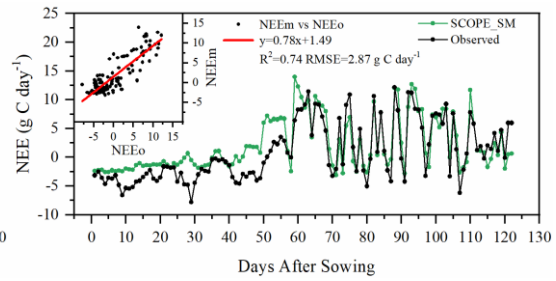
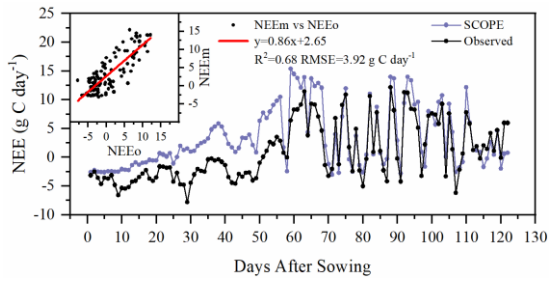
Simulated ~~NEEGPP~~ by SCOPE, SCOPE\_SM and ~~SCOPE\_STEMMUS-SCOPE~~ and observed ~~NEE were~~GPP are presented in Figure 10. As shown, similar to the simulation of transpiration, SCOPE cannot respond to water stress when simulating

370 ~~NEEGPP~~. After introducing soil water stress factor in ~~SCOPE\_STEMMUS-SCOPE~~ and SCOPE\_SM, the simulations of ~~NEEGPP~~ were improved in both models. For Yangling station, the consistency between simulated and observed ~~NEEGPP~~ at mid and late stages were higher than those at early and rapidly growth stages. The difference usually occurred when soil moisture increased. ~~The reason is that the simulated NEE was calculated by GPP and Re, and Re was not only influenced by soil temperature, but also by soil moisture. However, in this study, we only considered the effect of soil temperature on Re.~~

375 ~~Many studies evidenced that soil respiration increased with increasing soil moisture, especially when rain or irrigation occurred. Generally, in the summer, soil temperature decreases when raining or irrigating. However, the model only considers the effect of reduced soil temperature on Re, while ignores the positive effect of increasing soil moisture. As such, the simulated soil respiration would decrease with soil temperature dropped. For the late stage, as soil moisture was stable and maintained at a high level, the difference between simulated and observed soil respiration was relatively small. This can also demonstrate that~~

380 ~~the errors of NEE simulation were mainly caused by the effect of soil moisture on soil respiration. For US-Var site, STEMMUS-SCOPE can simulate GPP well during the whole period, while SCOPE SM slightly underestimated GPP around DOY 80 when this site transits from wet season to dry season. It indicates that only using the surface SM cannot reflect the actual root zone SM when the vegetation experiencing moderate water stress. Under such a condition, the hydraulic redistribution (HR) and compensatory root water uptake (CRWU) process enable the vegetation to utilize the water in deep soil layer. Only using~~

385 ~~the surface soil water content to calculate RWU in SCOPE\_SM ignored the effect of HR and CRWU process, and the effect of water stress was overestimated. However, the surface soil moisture can reflect root zone soil moisture well when the vegetation was not under water stress or severe water stress. A similar underestimated of GPP was also found by Bayat et al. (2019).~~



390

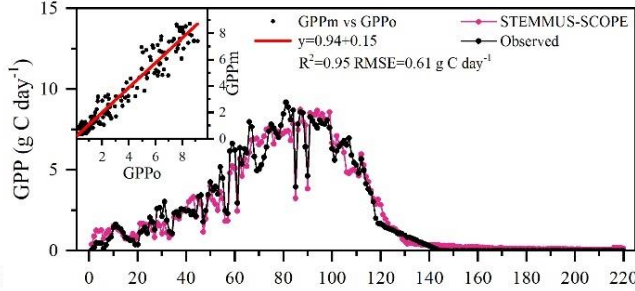
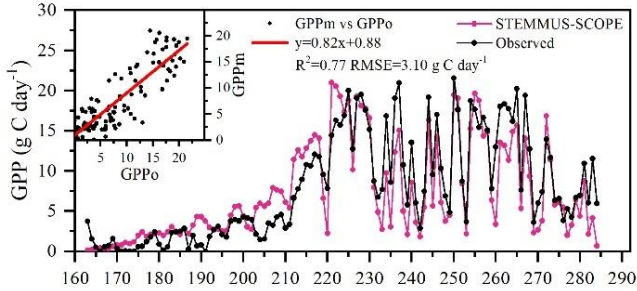
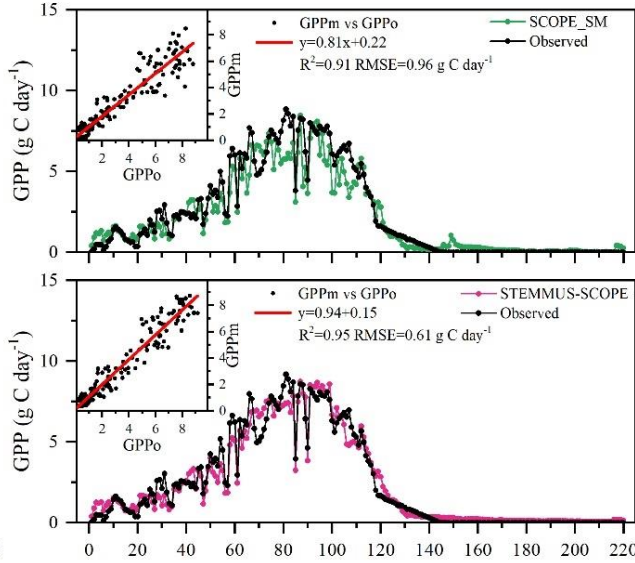
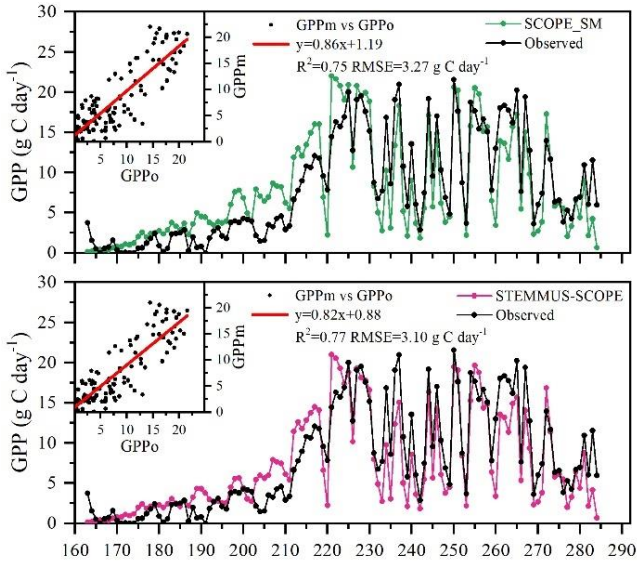
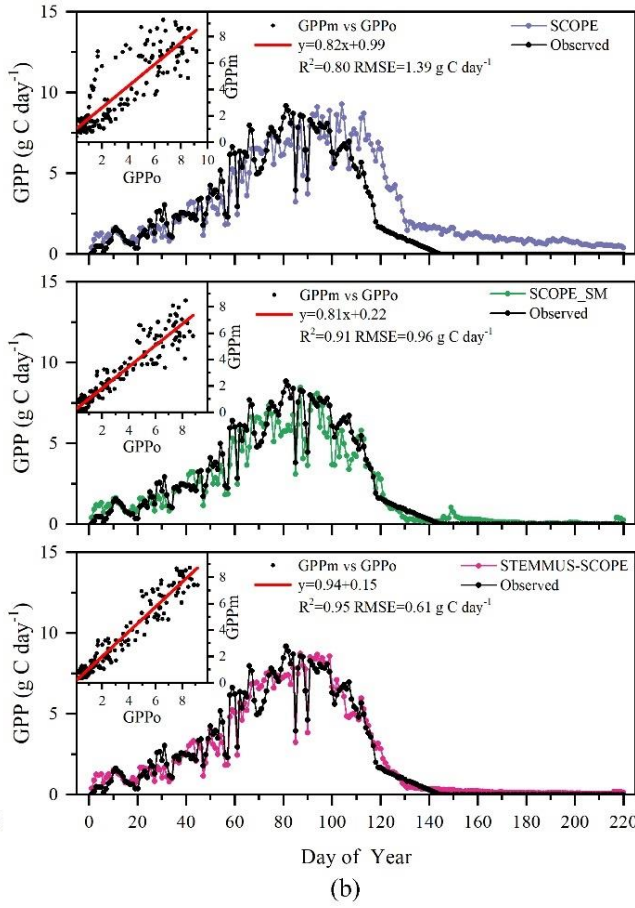
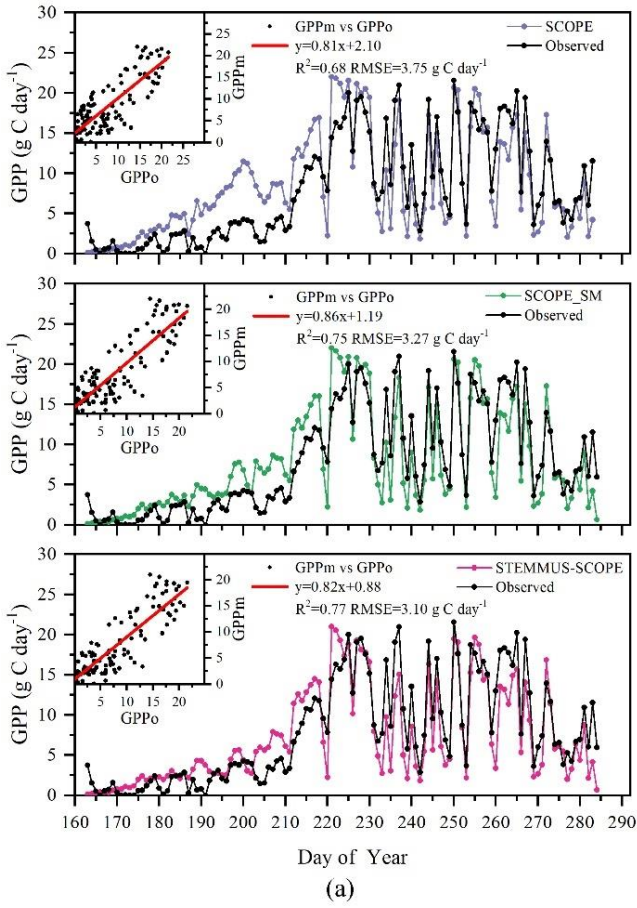


**Figure 10 Comparison of modeled and observed and modeled daily net ecosystem exchange (NEE) (NEE<sub>gross primary production</sub> (GPP): (a) Maize cropland at Yangling station; (b) Grassland at Vaira Ranch (US-Var) Fluxnet site. (GPP<sub>m</sub>: modeled GPP; GPP<sub>o</sub>: observed NEE; NEE<sub>m</sub>: modeled NEE; GPP).**

395 **4. Discussion**

**4.1.3.6. Simulation of leaf water potential, (LWP), water stress factor, (WSF), and root length density (RLD)**

Leaf water potential ~~was~~ a parameter to reflect plant water status. The simulated half-hourly leaf water potential and water stress factor ~~at Yangling station~~ are presented in Figure 11. The leaf water potential was lower when vegetation suffering water stress compared to other periods. The reason is that soil water potential is low due to the low soil moisture and the ~~leaves~~ plants need to maintain an even lower ~~leaf~~ water potential to suck water from the soil and transfer it to leaves. During mid and late stages, the leaf water potential was sensitive to transpiration demand due to the slowdown of root system growth. As the continuous measurements of the leaf water potential is not available, we compared ~~only~~ the ~~magnitude of~~ simulated leaf water potential to ~~the~~ measurements reported in ~~other literatures.~~ literature.

Many studies have measured midday leaf water potential or dawn leaf water potential. Fan et al. (2015) reported that the leaf water potential of well-watered maize was maintained high between -73 to -88 m and leaf water potential would decrease when soil water content was lower than 80% of field capacity. Martineau et al. (2017) reported the midday leaf water potential of well-watered maize was around -82 m and the midday leaf water potential decreased to -130 m when the maize was suffering water stress. Moreover, O'Toole and Cruz (1980) studied the response of leaf water potential to water stress in rice and concluded that the leaf water potential of rice can be lower than -80 to -120 m when the vegetation ~~is~~ was under water stress and the leaves ~~start~~ started curling, which was similar to the simulated leaf water potential of maize in this study. Aston and Lawlor (1979) revealed the relationship between transpiration, root water uptake and leaf water potential of maize. These field studies found that leaf water potential ~~is~~ was often very low and ~~it reaches valley~~ reached trough values at midday. Elfving (1972) developed a water flux model, ~~which was~~ based on SPAC system ~~and,~~ evaluated ~~with the~~ for orange tree. ~~In his study,~~ the valley, and reported about -120 m for the trough value of leaf water potential under non-limiting environmental conditions ~~was about -120 m,~~ which was slightly lower than the simulation in this study.

In this study, the calculation of water stress factor considered the effect of soil moisture and root distribution. The severe water stress ~~was~~ occurred from ~~DAS 30~~ DOY 193 to ~~DAS 40~~ DOY 202, and the coupled model performed very well in this period. As the feedback, water stress can also influence root water uptake and root growth, and ~~then~~ consequently influence soil moisture and root ~~dynamie~~ dynamics in ~~the~~ next time step. It indicates that the water stress equation used in this study can characterize the reduction of  $V_{cmax}$  reasonably well.

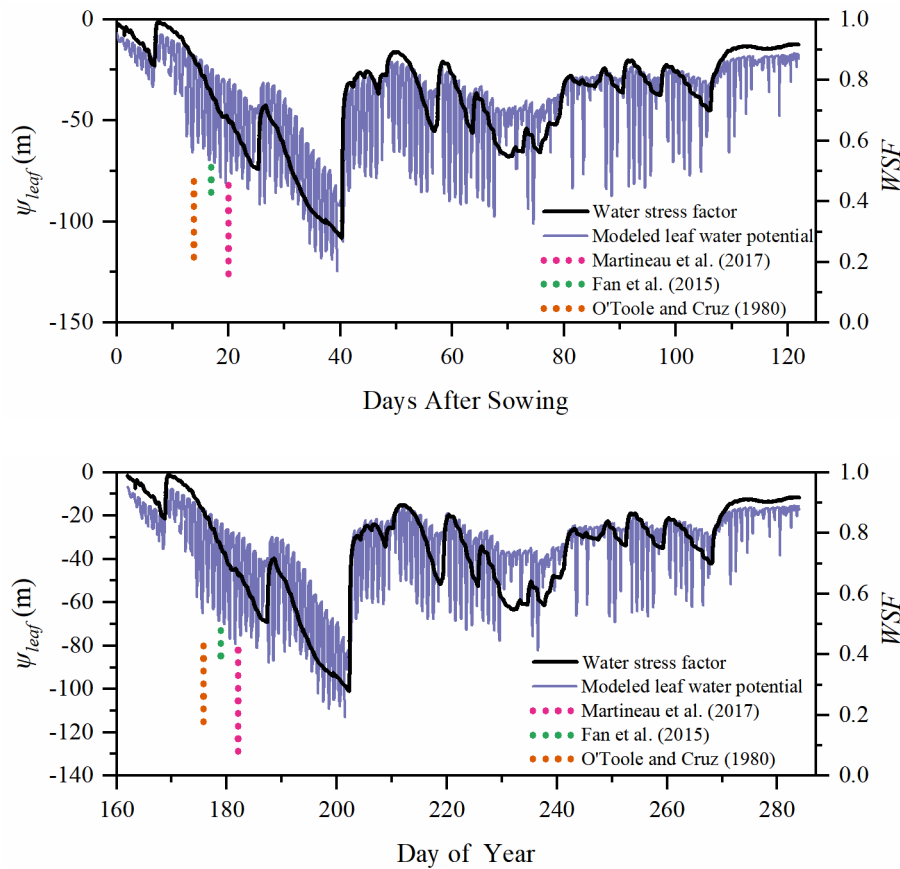
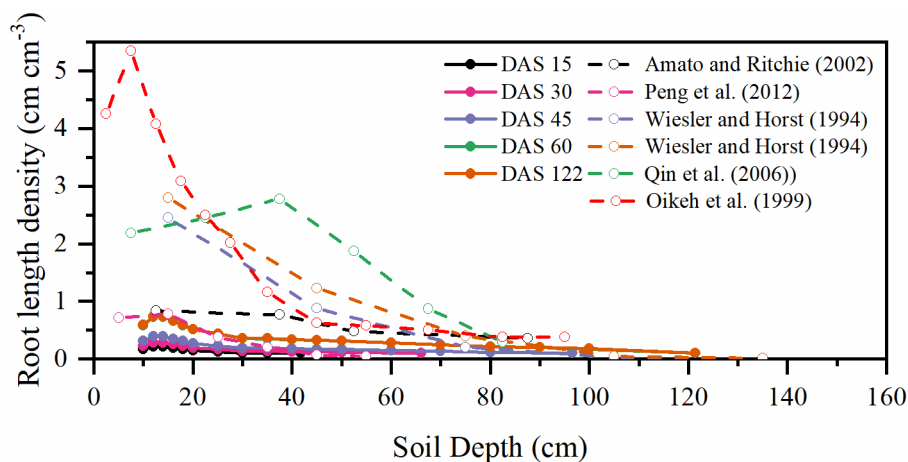


**Figure 11 Simulation of  $\psi_{leaf}$  (leaf water potential, m) and WSF (water stress factor) at Yangling station. (The dashed lines represent the range of midday leaf water potential reported in other sites.)**

425 Root length density is another vital parameter in calculating root water uptake ~~calculation~~. As shown in Figure 12 Table 3, the simulated peak root length density of maize at Yangling station was high in soil depth from 10 to 20 cm ~~depth~~ and gradually ~~decreased~~ ~~decreased~~ from 20 cm to 121 cm. Many previous studies ~~have~~ revealed that root length density was influenced by soil moisture, bulk density, tillage, and soil mineral nitrogen (Amato and Ritchie, 2002; Chassot et al., 2001; Schroder et al., 1996). In this study, as we assumed the soil was homogenous, SCOPE\_STEMMUS\_SCOPE considered the effect of soil moisture  
430 but neglected the effect of bulk density and soil mineral nitrogen.

Amato and Ritchie (2002) also found a similar result as this study about the root length density in a maize field. Peng et al. (2012) studied temporal and spatial dynamics in root length density of field-grown maize and found that 80% root length density was distributed at 0-30 cm depth with peak values from 0.86 to 1.00 cm cm<sup>-3</sup>. Ning et al. (2015) also reported a similar observation of root length density. Chassot et al. (2001) and Qin et al. (2006) reported that root length density can reach 71.59  
435 cm cm<sup>-3</sup> at Swiss midlands. Aina and Fapohunda (1986) also found that root length density can reach 2.5 cm cm<sup>-3</sup> if the maize

440 ~~was well-watered.~~ In Stuttgart, Germany, Wiesler and Horst (1994) observed the root growth and nitrate utilization of maize under field condition. The observed root length density was 2.45-2.80  $\text{cm cm}^{-3}$  at 0-30 cm depth which was much higher than in other studies, and decreased to 0.01  $\text{cm cm}^{-3}$  at 120-150 cm depth, which was consistent with the observation of Oikeh et al. (1999) at Samaru, Nigeria. Zhuang et al. (2001b) proposed a scaling model to estimate the distribution of root length density of field grown maize. In their study, measured root length density in Tokyo, Japan decreased from 0.4-0.95  $\text{cm cm}^{-3}$  at top soil layer to about 0.1  $\text{cm cm}^{-3}$  at the bottom layer. Zhuang et al. (2001a) observed that the root length density of maize was mainly distributed at 0-60 cm depth and the maximum values were about 0.9  $\text{cm cm}^{-3}$ . These studies ~~indicate~~indicated that the root length density values were quite variable when it was observed at different sites, nevertheless the simulated root length density in our study was in order of magnitude similar to the observations in previous studies- (Table 3).



445

**Figure 12 Simulation Table 3 Comparison of the peak root length density (RLD) ( $\text{cm cm}^{-3}$ ) at Yangling station with that at other sites.**

Location	Maximum rooting depth (cm)	Peak RLD ( $\text{cm cm}^{-3}$ )	Soil type	Bulk density ( $\text{g cm}^{-3}$ )	References
Potenza, Italy	100	0.84	Clay-loam	1.59-1.69	Amato and Ritchie (2002)
Beijing, China	60	0.78	Silty loam		Peng et al. (2012)
Alize, Stuttgart, Germany	150	2.45	Clay	1.5-1.7	Wiesler and Horst (1994)
Brummi, Stuttgart, Germany	150	2.80	Clay	1.5-1.7	Wiesler and Horst (1994)
Swiss midlands	100	1.59	Sandy silt	1.21-1.55	Qin et al. (2006)
Samaru, Nigeria	90	2.78	Loamy soil	1.39-1.67	Oikeh et al. (1999)
Tokyo, Japan	58	0.95	Sandy loam	0.61-0.80	Zhuang et al. (2001a, b)
Yangling, China	121	0.74	Sandy loam	1.41	This study

### 3.7. Diurnal variation of T, GPP, SIF, and LWP

450 Figure 12 shows the modeled and observed half-hourly canopy transpiration ( $T$ ), gross primary production ( $GPP$ ), solar-  
induced fluorescence ( $SIF$ ) and leaf water potential ( $LWP$ ) from DOY 183 to 202 at Yangling station. The dashed lines  
represent the measured simulations by STEMMUS-SCOPE and SCOPE\_SM were consistent with observation while that by  
SCOPE was much higher than observation. The performances of STEMMUS-SCOPE and SCOPE\_SM were consistent with  
that of SCOPE in the early morning and late afternoon, when the photosynthesis was mainly limited by incident radiation  
rather than by water stress, intercellular  $CO_2$  concentration and  $V_{cmax}$ . In the midday, with increasing incident radiation, the  
455 photosynthesis was mainly limited by water stress and  $V_{cmax}$ , exactly when the simulations by STEMMUS-SCOPE and  
SCOPE\_SM were much better than that by SCOPE. The diurnal variation of observed and modeled  $GPP$  were similar to that  
of  $T$ . Due to lack of observed  $SIF$ , only the simulated  $SIF$  were presented. As the figure shown, the  $SIF$  simulated by  
STEMMUS- SCOPE and SCOPE\_SM were reduced when the vegetation experiencing water stress, which indicated that both  
the simulated  $SIF$  of STEMMUS-SCOPE and SCOPE\_SM can respond to water stress. However, the accuracy of the simulated  
460  $SIF$  needs further validation with field observation.

Figure 13 shows the relationship among half-hourly  $GPP$ ,  $SIF$ , and  $LWP$  on DOY 199 at Yangling station. There was a strong  
linear relationship between  $SIF$  and  $GPP$  when the maize was well-watered (Figure 14a). However,  $SIF$  kept increasing while  
 $GPP$  tended to saturate when the maize suffering water stress. This result is consistent with the previous study conducted for  
cotton and tobacco leaves (Van der Tol et al., 2014). Because SCOPE\_SM used the averaged root length density zone SM and  
465 ignored vertical root and soil water distribution, it overestimated  $GPP$  and  $SIF$ . When the maize was experiencing drought, the  
 $LWP$  was maintained at a low level. With  $GPP$  and  $T$  increasing, the plant decreased  $LWP$  in order to extract enough water  
from the root zone. SPAC system enabled STEMMUS-SCOPE simulate half-hourly  $LWP$  and a liner relationship between the  
simulated  $SIF$  and  $LWP$  was obtained (Figure 14b). Sun et al. (2016) reported in other sites.)<sup>5</sup> that  $SIF$ -soil moisture-drought  
relationship depended on variations of both absorbed PAR and fluorescence yield in response to water stress, while the  $LWP$   
470 can reflect both effect of absorbed PAR and soil moisture status. The strong correlation between  $GPP$ ,  $LWP$  and  $SIF$  indicates  
a potential of using  $SIF$  as an effective signal for characterizing the response of photosynthesis to water stress. In the future,  
more studies should focus on the measurements of  $SIF$ ,  $GPP$ , and  $LWP$  simultaneously for different vegetation types across  
different environmental conditions (radiation, soil moisture, and  $CO_2$  concentration) to reveal how the water stress affects  
these relationships.

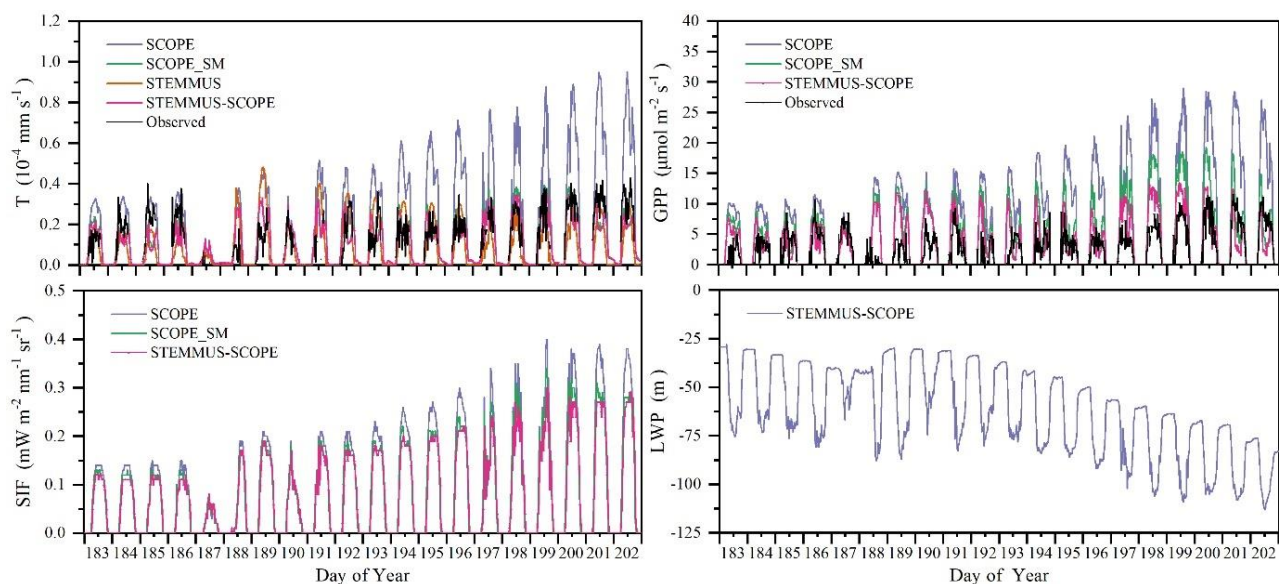
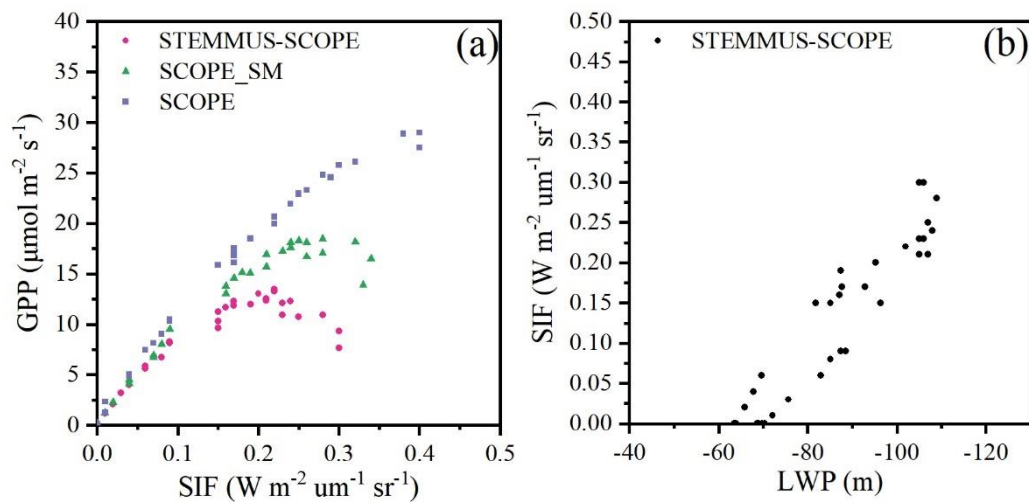


**Figure 12 Comparison of modeled and observed half-hourly transpiration (T), gross primary production (GPP), top of canopy solar-induced fluorescence (SIF) and leaf water potential (LWP) at Yangling station.**



**480 Figure 13 The relationship among gross primary production (GPP), top of canopy solar induced fluorescence (SIF), and leaf water potential (LWP) on DOY 199: (a) GPP vs SIF; (b) SIF vs LWP.**

### 3.8. Limitations need to be overcome

The new coupled model notably improved simulations of carbon and water fluxes when vegetation suffering water stress. However, this study mainly aimed to improve the response of SCOPE to drought by introducing vertical soil water and root profile. Some critical processes were followed that existed in SCOPE SM and STEMMUS. As with any model, some modules in STEMMUS-SCOPE, such as plant hydraulics and root growth, could be improved upon in future development.

First, to date many LSMs (e.g. CLM 5, Noah-MP, JULES, and CABLE) have incorporated state-of-the-art plant hydraulics model to replace the conventional empirical plant hydraulic model which was only based on the distribution of SM and fraction of roots (e.g. CLM 4.5 and CoLM) (De Kauwe et al., 2015). Although STEMMUS-SCOPE integrated a 1D root growth model and a relatively novel RWU model, its hydraulics model followed that in SCOPE SM and ignored the most exciting recent advances in our understanding of plant hydraulics: hydraulic failure due to loss of hydraulic conductivity due to embolism and refilling for recovery from xylem embolism (McDowell et al., 2019). Because STEMMUS-SCOPE performed well in maize cropland and grassland, the influence of embolism and refilling on water transfer from the soil through vegetation to the atmosphere cannot be fully detected. The value of using plant water potential instead of soil water potential to constrain model predictions has been demonstrated in many case studies (De Kauwe et al., 2020; Niu et al., 2020; Medlyn et al., 2016; Xu et al., 2016; Williams et al., 1996). Niu et al. (2020) followed the plant hydraulic model developed by Xu et al. (2016) and represented plant stomatal water stress factor as a function of the plant water storage. CLM 5.0 also introduced a new formulation for WSF, which is based on leaf water potential ( $\psi_l$ ) instead of soil water potential ( $\psi_s$ ) (Kennedy et al., 2019). These new formulations based on plant water potential could have significant improvements for plant drought responses. Besides, STEMMUS-SCOPE presently does not account for plant water storage that may result in underestimating morning LE and overestimating afternoon LE. Some field observations showed that the plant did not immediately respond when soil moisture was enhanced (Mackay et al., 2019), but there are long lags, which was ignored in this study too, between soil water recovery from drought and plant responses to the recovery. The WSF in STEMMUS-SCOPE directly comes from soil moisture and cannot reflect true stomatal response when vegetation experiencing drought. For example, in early morning, the low stomatal aperture was induced by low PAR rather than by SM. Consequently, STEMMUS-SCOPE needs to introduce the advanced hydraulics when the model was tested in a wide range of ecosystems, particularly for vegetation exposed to frequent drought cycles or prolonged periods of severe drought events. It is important however to note that explicit representations of plant hydraulics require additional model parameters and increase parameterization burden. This is the most challenging limitation to STEMMUS-SCOPE for incorporating these hydraulics models and we have chosen a trade-off between mechanism and practicality.

Second, as mentioned above, STEMMUS-SCOPE adapted the macroscopic RWU model and a simplified 1D root growth model for saving computational costs, though it well predicted root depth which is the most critical factor when calculating WSF and RWU. Such a simplification would likely ease the migration of our model into larger-scale models, such as earth

515 system models. However, STEMMUS-SCOPE oversimplified metabolic processes of the roots that include root exudates, root maintenance respiration, root growth respiration, and root turnover, which are also critical and have been incorporated in Noah-MP (Niu et al., 2020). This simplification could result in uncertainties in modelling the root growth and root water uptake. Furthermore, the model presently does not account for the feedback between hydraulic controls over carbon allocation and the role of root growth on soil-plant hydraulics, which could also be considered in future model development.

#### **4. Conclusions**

520 A fundamental understanding of coupled energy, water and carbon flux is vital for obtaining the information of ecohydrological processes and functioning under climate change. The coupled model, SCOPE-STEMMUS-SCOPE, integrating radiative transfer, photochemistry, energy balance, root system ~~dynamic~~dynamics, and soil moisture and soil temperature ~~dynamic~~dynamics, has been proven to be a practical model to simulate detailed land surface processes such as evapotranspiration and NEEGPP. In the coupled model, STEMMUS could provide root zone moisture profile to SCOPE, 525 which was used to calculate water stress factor. On the other hand, SCOPE can provide net carbon assimilation and soil surface temperature to STEMMUS, which was used subsequently as the top boundary condition. ~~The performance of and as the coupled SCOPE-STEMMUS~~input for root growth model. This study explores the role of dynamic root growth in ET partitioning was improved due to the comprehensive radiative transfer scheme in SCOPE, affecting canopy photosynthesis activities, fluorescence emissions and evapotranspiration, which has not been reported before. The coupled model has been 530 successfully applied in a maize field and a grassland, and can be used to describe ET partitioning, canopy photosynthesis, reflectance, and fluorescence emissions. The results show that via considering dynamic root growth and the associated root water uptake, the coupled STEMMUS-SCOPE model can reflect and capture realistically the SIF variation during water stress condition, while this is not the case for SCOPE and SCOPE SM.

Through the inter-comparison of SCOPE, SCOPE\_SM, STEMMUS, and SCOPE-STEMMUS-SCOPE, we concluded that the 535 coupled STEMMUS-SCOPE can be used to investigate vegetation states under water stress conditions, and to simultaneously understand the dynamics of soil heat and mass transfer, as well as the root growth. By considering vertical distribution of soil moisture and root system, the simulation of water and carbon fluxes, especially when vegetation suffering moderate water stress, was significantly improved. However, there ~~are~~remain some needs for further studies to enhance the capacity of STEMMUS-SCOPE in understanding ecosystem functioning. First of all, the estimation of soil boundary condition especially 540 during the irrigation period, which has significant influence on the simulation of soil temperature, needs further improvement considerations. Second, the soil respiration realism of the present model used in SCOPE, which neglected currently the effect of soil moisture, should be upgraded in the coupled model modelling water-stressed SIF are subject to further studies. Nevertheless, the SCOPE-STEMMUS-SCOPE may be used as an effective observation operator to simulate remote sensing signals and to assimilate remote sensing data such as solar-induced chlorophyll fluorescence, to improve the

545 estimation of water and carbon fluxes. SCOPE\_STEMMUS\_SCOPE could also be used to investigate regional or global land surface processes, especially in arid and semi-arid regions, due to its sensitivity to water stress conditions.

*Code and data availability.* The development and validation of SCOPE\_STEMMUS\_SCOPE in this paper were conducted in MATLAB R2016a. The exact version of the model used to produce the results used in this paper is archived on Zenodo (Wang et al., 2020). The original source of the SCOPE model and STEMMUS model was obtained from Van der Tol et al. (2009) and Zeng et al. (2011a, b), respectively. The tower-based eddy-covariance measurements used for model validation were obtained from the authors ~~in~~for the Yangling station, China (Wang et al., 2019); from the FLUXNET2015 Dataset and PLUMBER2 program for the Vaira Ranch (US-Var) Fluxnet site.

*Author contributions.* YW, YZ, ~~LY, PY, CV, ZS-HC~~ and HCZS designed the study, YW developed the code, conducted the analysis, and wrote the manuscript ~~with~~. YW and HC collected and shared their eddy-covariance measurements for the purpose of model validation. All authors ~~gave comments~~discussed, commented and contributed to the revisions and final version of the manuscript.

*Competing interests.* The authors declare that they have no conflict of interest.

*Acknowledgments.* This work was supported by the National Natural Science Foundation of China (51879223 and 41971033), the National Key Research and Development Program of China (2016YFC0400201), the Fundamental Research Funds for the Central Universities, CHD (300102298307), and China Scholarship Council. Peiqi Yang was supported by the Netherlands Organization for Scientific Research, grant ALWGO.2017.018.

## Appendix A

### A.1. ~~Water Stress Factor~~Photosynthesis and evapotranspiration under water stress in SCOPE

565 The C4 Photosynthesis is calculated in the SCOPE model as the minimum of three processes (~~FarquharCollatz et al., 1980~~1991; 1992); (1) carboxylation rate limited by Ribulose biphosphate-carboxylase-oxygenase activity (known as Rubisco (enzyme)-limited,  $V_c$ , described in Eq. (A1); (2) carboxylation rate limited by Ribulose 1–5 bisphosphate regeneration rate (known as RuBP (electron transport/light)-limited),  $V_e$ , described in Eq. (A2); (3) at low CO<sub>2</sub> concentrations, carboxylation rate limited by intercellular CO<sub>2</sub> partial pressure ( $p_i$ ),  $V_s$ , described in Eq. (A3).

$$V_c = V_{cmax} * WSF \quad (A1)$$

570  $V_e = \frac{J - b \pm \sqrt{b^2 - 4ac}}{6} \frac{1}{2a} \quad (A2)$

$$V_s = p_i(k_p - \frac{L}{p_i})/P \quad (A3)$$

$$A_n = \min(V_c, V_e, V_s) \quad (A4)$$

575 The C3 Photosynthesis is calculated in the SCOPE model as the minimum of two processes (Farquhar et al., 1980): (1) carboxylation rate limited by Ribulose biphosphate-carboxylase-oxygenase activity (known as Rubisco (enzyme)-limited,  $V_c$ , described in Eq. (A5); (2) carboxylation rate limited by Ribulose 1–5 bisphosphate regeneration rate (known as RuBP (electron transport/light)-limited),  $V_e$ , described in Eq. (A6).

$$V_c = V_{cmax} * WSF * \frac{C_i - \Gamma^*}{C_i + K_c(1 + \frac{O_i}{K_o})} \quad (A5)$$

$$V_e = \frac{J(C_i - \Gamma^*) - b \pm \sqrt{b^2 - 4ac}}{4(C_i + 2\Gamma^*)} \frac{1}{2a} \quad (A6)$$

$$A_n = \min(V_c, V_e) \quad (A7)$$

580  $C_i = C_a(1 - \frac{1}{mRH}) \quad (A5A8)$

where  $V_{cmax}$  is the maximum carboxylation rate ( $\mu\text{mol m}^{-2} \text{s}^{-1}$ ),  $p_i$  is the intercellular CO<sub>2</sub> partial pressure (Pa),  $k_p$  is a pseudo-first-order rate constant for PEP carboxylase with respect to  $C_i$ ,  $P$  is the atmospheric pressure;  $A_n$  is the net photosynthesis ( $\mu\text{mol m}^{-2} \text{s}^{-1}$ );  $WSF$  is the total water stress factor,  $J$  is the electron transport rate ( $\mu\text{mol m}^{-2} \text{s}^{-1}$ ),  $C_i$  is the intercellular CO<sub>2</sub> concentration ( $\mu\text{mol m}^{-3}$ ) and  $C_a$  is CO<sub>2</sub> concentration in the boundary layer ( $\mu\text{mol m}^{-3}$ ),  $m$  is Ball-Berry parameter and RH is relative humidity at the leaf surface (%).

585 In addition, leaf stomatal resistance  $r_c$  ( $\text{s m}^{-1}$ ) is calculated as:

$$r_c = \frac{0.625(C_s - C_i) \rho_a}{A_n} \frac{10^{12}}{M_a p} \quad (\text{A9})$$

Where  $\rho_a$  is specific mass of air ( $\text{kg m}^{-3}$ ),  $M_a$  is molecular mass of dry air ( $\text{g mol}^{-1}$ ), and  $p$  is atmosphere pressure (hPa).

The calculation of latent heat flux ( $LE$ ) is as follows:

$$590 \quad LE = \lambda \frac{(q_i - q_a)}{r_a + r_c} \quad (\text{A10})$$

Where  $\lambda$  is vaporization heat of water ( $\text{J kg}^{-1}$ ),  $q_i$  is the humidity in stomata or soil pores ( $\text{kg m}^{-3}$ ),  $q_a$  is the humidity above the canopy ( $\text{kg m}^{-3}$ ),  $r_c$  is stomatal or soil surface resistance ( $\text{s m}^{-1}$ ),  $r_a$  is aerodynamic resistance ( $\text{s m}^{-1}$ ).

In the study of Bayat et al. (2019), water stress factor was calculated based on the root zone soil moisture content neglecting the distribution of root length. In this study, water stress factor considered both root length distribution and water content in  
595 root zone. We use a sigmoid formulation rather than the piecewise function by Bayat et al. (2019). The calculations are as follows:

$$WSF = \sum_{i=1}^n RF(i) * WSF(i) \quad (\text{A6A11})$$

$$WSF(i) = \frac{1}{1 + e^{\frac{-100 + \theta_{sat} \left( SM(i) - \frac{\theta_f + \theta_w}{2} \right)}{1 + e^{\frac{-100 + \theta_{sat} \left( SM(i) - \frac{\theta_f + \theta_w}{2} \right)}}}} \quad (\text{A7A12})$$

600  $\theta_w$  is the soil water content at wilting point;  $\theta_f$  is the soil water content at field capacity;  $\theta_{sat}$  is the saturated soil water content;  $WSF(i)$  is the water stress factor at each soil layer;  $RF(i)$  is the ratio of root length in soil layer  $i$  and its calculation can be found in the appendix A.4;  $SM(i)$  is the soil moisture at each soil layer.

## A.2. Governing Equations in STEMMUS

### A.2.1 Soil water conservation equation

$$605 \quad \frac{\partial}{\partial t} (\rho_L \theta_L + \rho_V \theta_V) = - \frac{\partial}{\partial z} (q_{Lh} + q_{LT} + q_{La} + q_{Vh} + q_{VT} + q_{Va}) - S = \rho_L \frac{\partial}{\partial z} \left[ K \left( \frac{\partial h}{\partial z} + 1 \right) + D_{TD} \frac{\partial T_s}{\partial z} + \frac{K}{\gamma_w} \frac{\partial P_g}{\partial z} \right] + \frac{\partial}{\partial z} \left[ D_{Vh} \frac{\partial h}{\partial z} + D_{VT} \frac{\partial T_s}{\partial z} + D_{Va} \frac{\partial P_g}{\partial z} \right] - S \quad (\text{A8} \quad (\text{A13}))$$

where  $\rho_L$ ,  $\rho_V$  ( $\text{kg m}^{-3}$ ) are the density of liquid water, water vapor, respectively;  $q_L$ ,  $q_V$  ( $\text{m}^3 \text{m}^{-3}$ ) are the volumetric water content (liquid and water vapor, respectively);  $z$  (m) is the vertical space coordinate (positive upwards);  $S$  ( $\text{cm s}^{-1}$ ) is the sink term for the root water extraction.  $K$  ( $\text{m s}^{-1}$ ) is hydraulic conductivity;  $h$  (cm) is the pressure head;  $T_s$  ( $^{\circ}\text{C}$ ) is the soil temperature;  
610 and  $P_g$  (Pa) is the mixed pore-air pressure.  $\gamma_w$  ( $\text{kg m}^{-2} \text{s}^{-2}$ ) is the specific weight of water.  $D_{TD}$  ( $\text{kg m}^{-1} \text{s}^{-1} \text{ } ^{\circ}\text{C}^{-1}$ ) is the transport coefficient for adsorbed liquid flow due to temperature gradient;  $D_{Vh}$  ( $\text{kg m}^{-2} \text{s}^{-1}$ ) is the isothermal vapor conductivity; and  $D_{VT}$

( $\text{kg m}^{-1} \text{s}^{-1} \text{ } ^\circ\text{C}^{-1}$ ) is the thermal vapor diffusion coefficient.  $D_{Va}$  is the advective vapor transfer coefficient (Zeng et al. 2011a,b).  $q_{Lh}$ ,  $q_{LT}$ , and  $q_{La}$  ( $\text{kg m}^{-2} \text{s}^{-1}$ ) are the liquid water fluxes driven by the gradient of matric potential, temperature, and air pressure, respectively.  $q_{Vh}$ ,  $q_{VT}$ , and  $q_{Va}$  ( $\text{kg m}^{-2} \text{s}^{-1}$ ) are the water vapor fluxes driven by the gradient of matric potential, temperature, and air pressure, respectively.

### A.2.2 Dry air conservation equation

$$\frac{\partial}{\partial t} [\varepsilon \rho_{da} (S_a + H_c S_L)] = \frac{\partial}{\partial z} \left[ D_e \frac{\partial \rho_{da}}{\partial z} + \rho_{da} \frac{S_a K_g \partial P_g}{\mu_a \partial z} - H_c \rho_{da} \frac{q_L}{\rho_L} + (\theta_a D_{Vg}) \frac{\partial \rho_{da}}{\partial z} \right] \quad (\text{A9A14})$$

where  $\varepsilon$  is the porosity;  $\rho_{da}$  ( $\text{kg m}^{-3}$ ) is the density of dry air;  $S_a (=1-S_L)$  is the degree of air saturation in the soil;  $S_L (= \theta_L / \varepsilon)$  is the degree of saturation in the soil;  $H_c$  is Henry's constant;  $D_e$  ( $\text{m}^2 \text{s}^{-1}$ ) is the molecular diffusivity of water vapor in soil;  $K_g$  ( $\text{m}^2$ ) is the intrinsic air permeability;  $m_a$  ( $\text{kg m}^2 \text{s}^{-1}$ ) is the air viscosity;  $q_L$  ( $\text{kg m}^{-2} \text{s}^{-1}$ ) is the liquid water flux;  $\theta_a (= \theta_v - \theta_L)$  is the volumetric fraction of dry air in the soil; and  $D_{Vg}$  ( $\text{m}^2 \text{s}^{-1}$ ) is the gas phase longitudinal dispersion coefficient (Zeng et al., 2011a,b).

### A.2.3 Energy balance equation

$$\frac{\partial}{\partial t} [(\rho_s \theta_s C_s + \rho_L \theta_L C_L + \rho_V \theta_V C_V + \rho_{da} \theta_a C_a)(T_s - T_r) + \rho_V \theta_V L_0] - \rho_L W \frac{\partial \theta_L}{\partial t} = \frac{\partial}{\partial z} \left( \lambda_{eff} \frac{\partial T}{\partial z} \right) - \frac{\partial}{\partial z} [q_L C_L (T_s - T_r) + q_V (L_0 + C_V (T_s - T_r)) + q_a C_a (T_s - T_r)] - C_L S (T_s - T_r) \quad (\text{A10A15})$$

where  $C_s$ ,  $C_L$ ,  $C_V$ ,  $C_a$  ( $\text{J kg}^{-1} \text{ } ^\circ\text{C}^{-1}$ ) are the specific heat capacities of solids, liquid, water vapor, and dry air, respectively;  $\rho_s$  ( $\text{kg m}^{-3}$ ),  $\rho_L$  ( $\text{kg m}^{-3}$ ),  $\rho_V$  ( $\text{kg m}^{-3}$ ), and  $\rho_{da}$  ( $\text{kg m}^{-3}$ ) are the density of solids, liquid water, water vapor, and dry air, respectively;  $\theta_s$  is the volumetric fraction of solids in the soil;  $\theta_L$ ,  $\theta_V$ , and  $\theta_a$  are the volumetric fraction of liquid water, water vapor, and dry air, respectively;  $T_r$  ( $^\circ\text{C}$ ) is the reference temperature;  $L_0$  ( $\text{J kg}^{-1}$ ) is the latent heat of vaporization of water at temperature  $T_r$ ;  $W$  ( $\text{J kg}^{-1}$ ) is the differential heat of wetting (the amount of heat released when a small amount of free water is added to the soil matrix); and  $\lambda_{eff}$  ( $\text{W m}^{-1} \text{ } ^\circ\text{C}^{-1}$ ) is the effective thermal conductivity of the soil;  $q_L$ ,  $q_V$ , and  $q_a$  ( $\text{kg m}^{-2} \text{s}^{-1}$ ) are the liquid, vapor water and dry air flux.

## A.3. Dynamic Root Growth Modelling

### A.3.1. Root front growth

The depth of the root front is firstly initialized either with the sowing depth for sown crops or with an initial value for transplanted crops or perennial crops. The root front growth stops when it reached certain depth of soil or a physical/chemical obstacle preventing root growth, but also stops when the phenological stopping stage has been reached.

$$\Delta Z = \begin{cases} 0 & T_{air} < T_{min} \\ (T_{air} - T_{min}) * RGR & T_{min} < T_{air} < T_{max} \\ (T_{max} - T_{min}) * RGR & T_{max} < T_{air} \end{cases}$$

(A11A16)

640  $D_Z(t) = D_Z(t - 1) + \Delta Z$

(A12A17)

where  $\Delta Z$  is root front growth at  $t$ -th time step;  $D_Z$  (cm) is root zone depth;  $T_{air}$  ( $^{\circ}\text{C}$ ) is air temperature;  $T_{min}$  ( $^{\circ}\text{C}$ ) is the minimum temperature offor root growth;  $T_{max}$  ( $^{\circ}\text{C}$ ) is the maximum temperature offor root growth;  $RGR$  ( $\text{cm } ^{\circ}\text{C}^{-1} \text{ day}^{-1}$ ) is the root growth rate of root front.

### 645 A.3.2. Root length growth

In this study, the root distribution in the root zone was realized via simulating the root length growth in each soil layer.

$$\Delta RL_{tot} = \frac{A_n * fr_{root}}{R_C * R_D * \pi * r_{root}^2}$$

(A13A18)

650  $fr_{root}$  is the allocation fraction of net assimilation to root, and  $fr_{root}$  is assumed as a function of leaf area index (LAI) and root zone water content.  $A_n$  is the net assimilation rate ( $\mu\text{mol m}^{-2} \text{ s}^{-1}$ ).  $R_C$  is ratio of carbon to dry organic matter in root,  $R_D$  is root length density ( $\text{g m}^{-3}$ ), and  $r_{root}$  is radius of the root ( $0.15 * 10^{-3} \text{ m}$ ), and  $\Delta RL_{tot}$  ( $\text{m m}^{-3}$ ) is total root length growth.

The limiting factors for allocation are preliminarily computed and they account for root zone soil moisture availability  $A_W$ , and light availability  $A_L$ .

655  $A_W = \max[0.1, \min(1, WSF)]$

(A14A19)

where  $WSF$  is the averaged soil moisture stress factor in the root zone.

$$A_L = \max[0.1, e^{-K_e LAI}]$$

(A15A20)

where  $K_e = 0.15$  is a constant light extinction coefficient.

660  $fr_{root} = \max \left[ r_{min}, r_0 \frac{3A_L}{A_L + 2A_W} \right]$

(A16A21)

where  $r_{min}(= 0.15)$  is the minimum allocation coefficient to fine roots, and  $r_0$  is a coefficient that indicates the theoretically unstressed allocation to fine roots.

$$\Delta RL(i) = \Delta RL_{tot} * RF(i)$$

(A17A22)

where  $RF(i)$  is the allocation fraction of root growth length in layer  $i$ ,  $\Delta RL(i)$  is the root growth length in layer  $i$ .

For  $i = 1$  to  $n-1$  ( $i = 1$  means the top soil layer):

$$RL_i^t = RL_i^{t-1} + \Delta RL(i) \quad (A18(i))$$

(A23)

For  $i = n$ :

$$RL_i^t = RL_i^{t-1} + \Delta RL(i) + RL_{front} \quad (A24)$$

where  $RL_i^t$  and  $RL_i^{t-1}$  is the root length of layer  $i$  at time step  $t$  and time step  $t-1$ .

$$RF(i) = \frac{RL(i)}{RL_T}$$

(A19A25)

where  $RL_T$  is the total root length in root zone,  $RL(i)$  is the root length in soil layer  $i$ .

At the root front, the density is imposed and estimated by the parameter  $L_{v\_front}$  and the growth in root length depends directly on the root front growth rate  $\Delta Z$ :

$$RL_{front} = L_{v\_front} * \Delta Z \quad (A26)$$

#### A.4. Root water uptake

The equation to calculate root water uptake and transpiration was as follows:

$$\sum_{i=1}^n \frac{\psi_{s,i} - \psi_l}{r_{s,i} + r_{r,i} + r_{x,i}} = \frac{0.622}{P} \frac{\rho_{da}}{\rho_V} \left( \frac{e_l - e_a}{r_c + r_a} \right) = T$$

(A20A27)

where  $\psi_{s,i}$  is soil water potential of layer  $i$  (m),  $\psi_l$  is leaf water potential (m),  $r_{s,i}$  is the soil hydraulic resistance ( $s \text{ m}^{-1}$ ),  $r_{r,i}$  is the root resistance to water flow radially across the roots ( $s \text{ m}^{-1}$ ), and  $r_{x,i}$  is the plant axial resistance to flow from the soil to the leaves ( $s \text{ m}^{-1}$ ).  $e_l$  and  $e_a$  are vapor pressure of leaf and the atmosphere (hPa), respectively, and  $r_a$  and  $r_c$  are aerodynamic

resistance and canopy resistance ( $s\ m^{-1}$ ), respectively.  $\rho_{da}$  is the density of dry air ( $kg\ m^{-3}$ ).  $\rho_v$  is the density of water vapor.  $P$  is the atmospheric pressure (Pa). 0.622 is the ratio of the molar mass of water to air.

$\psi_{s,i}$  is described as a function of soil moisture by Van Genuchten (1980), and the relevant parameters were shown in Table B.1.

690 The  $r_s$  is calculated by Reid and Huck (1990) as:

$$r_s = \frac{1}{B \cdot K \cdot R_D \cdot \Delta d} + \frac{1}{B \cdot K \cdot L_v \cdot \Delta d} \quad (A21)$$

(A28)

where  $B$  is the root length activity factor,  $K$  is hydraulic conductivity of soil ( $m\ s^{-1}$ ),  $R_D L_v$  is root length density ( $m\ m^{-3}$ ), and  $\Delta d$  is the thickness of the soil layer (m).  $B$  is calculated as:

695

$$B = \frac{2\pi}{\ln[(\pi R_D)^{-1/2} / r_{root}]}$$

(A22A29)

where  $r_{root}$  is root radius (m).

The  $r_r$  is estimated as (Reid and Huck, 1990):

700

$$r_r = \frac{P_r (\theta_{sat} / \theta)}{L_v \Delta d}$$

(A23A30)

where  $P_r$  is root radial resistivity ( $s\ m^{-1}$ ).

The xylem resistance  $r_x$  is estimated by Klepper et al. (1983):

$$r_x = \frac{P_a Z_{mid}}{0.5 f L_v}$$

(A24A31)

705 where  $P_a$  is root axial resistivity ( $s\ m^{-3}$ ),  $Z_{mid}$  is the depth of the midpoint of soil layer, and  $f$  is a fraction defined for a specific depth as the number of roots which connect directly to the stem base to total roots crossing a horizontal plane at that depth. We can consider it equal to 0.22 based on Klepper et al. (1983).

The updated root water uptake term is:

$$S_i = \frac{\psi_{s,i} - \psi_l}{r_{s,i} + r_{r,i} + r_{x,i}}$$

(A25A32)

710

Different from other studies which need to calculate the ~~compensatory~~ compensatory water uptake and hydraulic redistribution after calculating the standard water uptake of each soil layer, the sink term in this study is calculated by a physically-based model which contain the effect of root resistance and soil hydraulic resistance rather than only considering the root fraction, so the ~~compensary~~ compensatory water uptake and hydraulic redistribution have been considered when ~~ealeuating~~ calculating the sink term.

715

## Appendix B.

**Table B.1 List of parameters and values used in this study (All the parameters were classified as Air, Canopy, Root and Soil).**

Symbol	Description	Unit	Value	
			Maize	Grass
<b>Aerodynamic</b>				
<i>aPAR</i>	Absorbed photosynthetically active radiation	$\mu\text{mol m}^{-2} \text{s}^{-1}$		
<i>e<sub>a</sub></i>	Air vapor pressure	Pa		
<i>e<sub>l</sub></i>	Vapor pressure of leaf	hPa		
<i>P</i>	Air pressure	Pa		
<i>q<sub>a</sub></i>	Humidity above the canopy	$\text{kg m}^{-3}$		
<i>q<sub>l</sub></i>	Humidity in stomata	$\text{kg m}^{-3}$		
<i>r<sub>a</sub></i>	Aerodynamic resistance	$\text{s m}^{-1}$		
<i>RH</i>	Relative humidity	%		
<i>R<sub>li</sub></i>	Incoming longwave radiation	$\text{W m}^{-2}$		
<i>R<sub>in</sub></i>	Incoming shortwave radiation	$\text{W m}^{-2}$		
<i>R<sub>n</sub></i>	Net radiation	$\text{W m}^{-2}$		
<i>T<sub>air</sub></i>	Air temperature	$^{\circ}\text{C}$		
<i>u</i>	Wind speed	$\text{m s}^{-1}$		
<i>VPD</i>	Vapor pressure deficit	hPa		
<b>Canopy</b>				
<i>A<sub>n</sub></i>	Net assimilation rate	$\mu\text{mol m}^{-2} \text{s}^{-1}$		
<i>C<sub>a</sub></i>	CO <sub>2</sub> concentration in the boundary layer	$\mu\text{mol m}^{-3}$		
<i>C<sub>ab</sub></i>	Leaf chlorophyll content	$\mu\text{g cm}^{-2}$	80	0.374-50.45
<i>C<sub>ca</sub></i>	Leaf Carotenoid content	$\mu\text{g cm}^{-2}$	20	0.25* <i>C<sub>ab</sub></i>
<i>C<sub>w</sub></i>	Leaf water content	$\text{g cm}^{-2}$	0.009	.002
<i>C<sub>dm</sub></i>	Leaf dry matter content	$\text{g cm}^{-2}$	0.012	0.015
<i>C<sub>s</sub></i>	Senescent material content		0	0
<i>DOY</i>	Day of Year	d		
<i>ET</i>	Evapotranspiration	$\text{mm day}^{-1}$		
<i>GPP</i>	Gross primary production	$\text{g C m}^{-2} \text{day}^{-1}$		
<i>h<sub>c</sub></i>	Canopy height	m	0-1.95	0.55
<i>H</i>	Sensible heat flux	$\text{W m}^{-2}$		
<i>J</i>	Electron transport rate	$\mu\text{mol m}^{-2} \text{s}^{-1}$		

$K_e$	Light extinction coefficient		0.15	0.15
$k_p$	A pseudo-first-order rate constant for PEP carboxylase			
LAI	Leaf area index	$\text{m}^2 \text{m}^{-2}$	0-4.39	0.745-2.03
LIDF	Leaf inclination distribution function		-1, 0	0.08, -0.15
LE	Latent heat flux	$\text{W m}^{-2}$		
LE <sub>c</sub>	Latent heat flux of canopy	$\text{W m}^{-2}$		
$m$	Ball-Berry stomatal conductance parameter		4	10
NEE	Net ecosystem exchange	$\text{g C m}^{-2} \text{day}^{-1}$		
$p_i$	Intercellular CO <sub>2</sub> partial pressure	Pa		
$r_c$	Canopy resistance	$\text{s m}^{-1}$		
Re	Ecosystem respiration	$\text{g C m}^{-2} \text{day}^{-1}$		
T	Transpiration	$\text{mm day}^{-1}$		
$T_c$	Vegetation temperature	$^{\circ}\text{C}$		
$T_{ch}$	Leaf temperature (shaded leaves)	$^{\circ}\text{C}$		
$T_{cu}$	Leaf temperature (sunlit leaves)	$^{\circ}\text{C}$		
$uWUE_p$	Potential water use efficiency	$\text{g C hPa}^{0.5}/\text{kg H}_2\text{O}$		
$uWUE$	Water use efficiency	$\text{g C hPa}^{0.5}/\text{kg H}_2\text{O}$		
$V_{cmax}$	Maximum carboxylation rate	$\mu\text{mol m}^{-2} \text{s}^{-1}$	50	10.7-100.3
$\psi_l$	Leaf water potential	m		
<b>Root</b>				
$A_w$	Root zone soil moisture availability			
$A_L$	Light availability			
B	Root length activity factor			
$D_z$	Root zone depth	cm		
f	A fraction defined for a specific depth as the number of roots which connect directly to the stem base to total roots crossing a horizontal plane at that depth		0.22	0.22
$f_{r_{root}}$	Allocation fraction of net assimilation to root			
$P_a$	Root axial resistivity	$\text{s m}^{-3}$	$0.65*10^{12}$	$2*10^{12}$
$P_r$	Root radial resistivity	$\text{s m}^{-1}$	$1*10^{10}$	$1.2*10^{11}$
RF(i)	The allocation fraction of root growth length in layer i			

$RL_T$	Total root length in root zone	$m\ m^{-2}$		
$RL_i^t$	Root length of layer $i$ at time step $t$	$m\ m^{-2}$		
$RL_i^{t-1}$	Root length of layer $i$ at time step $t-1$	$m\ m^{-2}$		
$RL(i)$	Root length in soil layer $i$	$m\ m^{-2}$		
$RL_{front}$				
$RGR$	Root growth rate of front	$cm\ ^\circ C\ day^{-1}$	0.096	0.072
$R_D$	Root density	$g\ m^{-3}$	250000	250000
$L_v$	Root length density	$m\ m^{-3}$		
$L_{v\_front}$	Root density at the root front	$m\ m^{-3}$	1000	150
$r_{min}$	The minimum allocation coefficient to fine roots		0.15	0.15
$r_0$	Coefficient of theoretically unstressed allocation to fine roots		0.3	0.3
$r_{root}$	Radius of the root	$m$	$0.15*10^{-3}$	$1.5*10^{-3}$
$r_{x,i}$	Plant axial resistance to flow from the soil to the leaves	$s$		
$r_{r,i}$	Resistance to water flow radially across the roots	$s$		
$r_{s,i}$	Soil hydraulic resistance	$s$		
$R_C$	Ratio of carbon to dry organic matter in root	$kg\ kg^{-1}$	0.488	0.488
RWU	Root water uptake	$m\ s^{-1}$		
$RF(i)$	The ratio of root length in soil layer $i$			
$T_{min}$	Minimum temperature of root growth	$^\circ C$	10	0
$T_{max}$	Maximum temperature of root growth	$^\circ C$	40	40
$\Delta Z$	Root front growth at $t$ -th step	$cm$		
$\Delta RL_{tot}$	Total root length growth	$m$		
$\Delta RL(i)$	The root growth length in layer $i$	$m$		
<b>Soil</b>				
$C_s$	Specific heat capacities of solids	$J\ kg^{-1}\ ^\circ C^{-1}$		
$C_L$	Specific heat capacities of liquid	$J\ kg^{-1}\ ^\circ C^{-1}$	$4.186*10^3$	$4.186*10^3$
$C_V$	Specific heat capacities of water vapor	$J\ kg^{-1}\ ^\circ C^{-1}$	$1.870*10^3$	$1.870*10^3$
$C_a$	Specific heat capacities of dry air	$J\ kg^{-1}\ ^\circ C^{-1}$	$1.255*10^3$	$1.255*10^3$
$D_{TD}$	Transport coefficient for absorbed liquid flow due to temperature gradient	$kg\ m^{-1}\ s^{-1}\ ^\circ C^{-1}$		
$D_{Vh}$	Isothermal vapor conductivity	$kg\ m^{-2}\ s^{-1}$		

$D_{VT}$	Thermal vapor diffusion coefficient	$\text{kg m}^{-1} \text{s}^{-1} \text{ } ^\circ\text{C}^{-1}$		
$D_{Va}$	Advective vapor transfer coefficient	$\text{kg m}^{-2} \text{s}^{-1}$		
$D_{Vg}$	Gas phase longitudinal dispersion coefficient	$\text{m}^2 \text{s}^{-1}$		
$D_e$	Molecular diffusivity of water vapor in soil	$\text{m}^2 \text{s}^{-1}$		
$E$	Soil evaporation	mm		
$G$	Soil heat flux	$\text{W m}^{-2}$		
$h$	Soil matric potential	cm		
$H_c$	Henry's constant		0.02	0.02
$K$	Hydraulic conductivity	$\text{m s}^{-1}$		
$K_g$	Intrinsic air permeability	$\text{m}^2$		
$K_s$	Saturation hydraulic conductivity	$\text{cm day}^{-1}$	18	10
$LE_s$	Latent heat flux of soil	$\text{W m}^{-2}$		
$L_0$	Latent heat of vaporization of water temperature $T_r$	$\text{J kg}^{-1}$	2497909	2497909
$m_a$	Air viscosity	$\text{kg m}^{-1} \text{s}^{-1}$	$1.846 \times 10^{-5}$	$1.846 \times 10^{-5}$
$n$	Soil-dependent parameter		1.41	1.50
$P_g$	Mixed pore-air pressure	Pa		
$q_L$	Liquid water flux	$\text{kg m}^{-2} \text{s}^{-1}$		
$q_{Lh}$	Liquid water flux driven by the gradient of matric potential	$\text{kg m}^{-2} \text{s}^{-1}$		
$q_{LT}$	Liquid water flux driven by the gradient of temperature	$\text{kg m}^{-2} \text{s}^{-1}$		
$q_{La}$	Liquid water flux driven by the gradient of air pressure	$\text{kg m}^{-2} \text{s}^{-1}$		
$q_V$	Water vapor flux	$\text{kg m}^{-2} \text{s}^{-1}$		
$q_{Vh}$	Water vapor flux driven by the gradient of matric potential	$\text{kg m}^{-2} \text{s}^{-1}$		
$q_{VT}$	Water vapor flux driven by the gradient of temperature	$\text{kg m}^{-2} \text{s}^{-1}$		
$q_{Va}$	Water vapor flux driven by the gradient of air pressure	$\text{kg m}^{-2} \text{s}^{-1}$		
$q_a$	Dry air flux	$\text{kg m}^{-2} \text{s}^{-1}$		
$S$	Sink term for the root water extraction	$\text{cm s}^{-1}$		
$S_a$	Degree of air saturation in the soil			
$S_L$	Degree of saturation in the soil			
$SM(i)$	The soil moisture at a specific soil layer	$\text{m}^3 \text{m}^{-3}$		
$T_s$	Soil temperature	$^\circ\text{C}$		
$T_{s0}$	Soil surface temperature	$^\circ\text{C}$		

$T_r$	Reference temperature	°C	20	20
$W$	Differential heat of wetting	J kg <sup>-1</sup>	1.001*10 <sup>3</sup>	1.001*10 <sup>3</sup>
$WSF$	Total water stress factor			
$WSF(i)$	Water stress factor at a specific soil layer			
$Z_{mid}$	The depth of the midpoint of soil layer	m		
$\Delta d$	Thickness of the soil layer	m		
$\alpha$	Soil-dependent parameter	m <sup>-1</sup>	0.45	0.166
$\theta_{sat}$	Saturated water content	m <sup>3</sup> m <sup>-3</sup>	0.42	0.38
$\theta_f$	Field capacity	m <sup>3</sup> m <sup>-3</sup>	0.272	0.24
$\theta_w$	Wilting point	m <sup>3</sup> m <sup>-3</sup>	0.10	0.03
$\theta_r$	Residual water content	m <sup>3</sup> m <sup>-3</sup>	0.0875	0.0008
$\theta$	Volumetric soil water content	m <sup>3</sup> m <sup>-3</sup>		
$\theta_L$	Volumetric moisture content	m <sup>3</sup> m <sup>-3</sup>		
$\theta_V$	Volumetric vapor content	m <sup>3</sup> m <sup>-3</sup>		
$\theta_s$	Volumetric fraction of solids in the soil	m <sup>3</sup> m <sup>-3</sup>		
$\theta_a$	Volumetric fraction of dry air in the soil	m <sup>3</sup> m <sup>-3</sup>		
$\psi_{s,i}$	Soil water potential of layer $i$	m		
$\psi_{soil}$	Soil water potential	m		
$\lambda_{eff}$	Effective thermal conductivity of the soil	W m <sup>-1</sup> °C <sup>-1</sup>		
$\gamma_w$	Specific weight of water	kg m <sup>-2</sup> s <sup>-2</sup>		
$\rho_{da}$	Density of dry air	kg m <sup>-3</sup>		
$\rho_V$	Density of vapor	kg m <sup>-3</sup>		
$\rho_L$	Density of liquid water	kg m <sup>-3</sup>	1	1
$\rho_s$	Density of solids	kg m <sup>-3</sup>		
$\varepsilon$	Soil porosity	m <sup>3</sup> m <sup>-3</sup>	0.50	0.50

720 **References**

- ~~Aina, P. and Fapohunda, H.: Root distribution and water uptake patterns of maize cultivars field grown under differential irrigation, *Plant Soil*, 94, 257-265, <https://doi.org/10.1007/bf02374349>, 1986.~~
- Amato, M. and Ritchie, J.T.: Spatial distribution of roots and water uptake of maize (*Zea mays* L.) as affected by soil structure, *Crop Sci.*, 42, 773-780, <https://doi.org/10.2135/cropsci2002.7730>, 2002.
- 725 Amenu, G. and Kumar, P.: A model for hydraulic redistribution incorporating coupled soil-root moisture transport, *Hydrol. Earth Syst. Sci.*, 4, 3719-3769, <https://doi.org/10.5194/hessd-4-3719-2007>, 2007.
- Aston, M. and Lawlor, D.W.: The relationship between transpiration, root water uptake, and leaf water potential, *J. Exp. Bot.*, 30, 169-181, <https://doi.org/10.1093/jxb/30.1.169>, 1979.
- Bayat, B., Van der Tol, C., and Verhoef, W.: Integrating satellite optical and thermal infrared observations for improving daily ecosystem functioning estimations during a drought episode, *Remote Sens. Environ.*, 209, 375-394, <https://doi.org/10.1016/j.rse.2018.02.027>, 2018.
- 730 Bayat, B., Van der Tol, C., Yang, P., and Verhoef, W.: Extending the SCOPE model to combine optical reflectance and soil moisture observations for remote sensing of ecosystem functioning under water stress conditions, *Remote Sens. Environ.*, 221, 286-301, <https://doi.org/10.1016/j.rse.2018.11.021>, 2019.
- 735 Beaudoin, N., Mary, B., Launay, M., and Brisson, N.: Conceptual basis, formalisations and parameterization of the STICS crop model, *Quae*, 2009.
- Bingham, I.J. and Wu, L.: Simulation of wheat growth using the 3D root architecture model SPACSYS: validation and sensitivity analysis, *Eur. J. Agron.*, 34, 181-189, <https://doi.org/10.1016/j.eja.2011.01.003>, 2011.
- Caldwell, M.M., Dawson, T.E., and Richards, J.H.: Hydraulic lift: consequences of water efflux from the roots of plants, *Oecologia*, 113, 151-161, <https://doi.org/10.1007/s004420050363>, 1998.
- 740 Camargo, G. and Kemanian, A.: Six crop models differ in their simulation of water uptake, *Agric. For. Meteorol.*, 220, 116-129, <https://doi.org/10.1016/j.agrformet.2016.01.013>, 2016.
- Chassot, A., Stamp, P., and Richner, W.: Root distribution and morphology of maize seedlings as affected by tillage and fertilizer placement, *Plant Soil*, 231, 123-135, <https://doi.org/10.1023/A:1010335229111>, 2001.
- 745 [Collatz G J, Ball J T, Grivet C et al. Physiological and environmental regulation of stomatal conductance, photosynthesis and transpiration, \*Agric. For. Meteorol.\* 54\(2/3/4\): 107-136, \[https://doi.org/10.1016/0168-1923\\(91\\)90002-8\]\(https://doi.org/10.1016/0168-1923\(91\)90002-8\), 1991](#)

Collatz G J, Ribas-Carbo M, Berry J A.: Coupled photosynthesis-stomatal conductance model for leaves of C4 plants. Australian Journal of Plant Physiology, 19: 519-538, 1992

750 Couvreur, V., Vanderborght, J., and Javaux, M.: A simple three-dimensional macroscopic root water uptake model based on the hydraulic architecture approach, *Hydrol. Earth Syst. Sci.*, 16, 2957-2971, <https://doi.org/10.5194/hess-16-2957-2012>, 2012.

De Kauwe, M.G., Medlyn, B.E., Ukkola, A.M., Mu, M., Sabot, M.E., Pitman, A.J., Meir, P., Cernusak, L., Rifai, S.W., Choat, B., Tissue, D.T., Blackman, C.J., Li, X., Roderick, M. and Briggs, P.R.: Identifying areas at risk of drought-induced tree mortality across SouthEastern Australia. *Glob. Change Biol.*, <https://doi.org/10.1111/gcb.15215>, 2020.

755 De Kauwe, M.G., Zhou, S.X., Medlyn, B.E., Pitman, A.J., Wang, Y.P., Duursma, R.A., and Prentice I.C.: Do land surface models need to include differential plant species responses to drought? examining model predictions across a mesic-xeric gradient in Europe. *BIOGEOENCES*, 2015,12(24), 7503-7518, <https://doi.org/10.5194/bg-12-7503-2015>, 2015.

Deng, Z., H. Guan, J. Hutson, M. A. Forster, Y. Wang, and C. T. Simmons.: A vegetation focused soil-plant-atmospheric continuum model to study hydrodynamic soil-plant water relations, *Water Resour. Res.*, 53, 4965– 4983, <https://doi.org/10.1002/2017WR020467>, 2017.

760 Elfving, D. C., KAUFMANN, M. R., and HALL, A. E.: Interpreting leaf water potential measurements with a model of the soil-plant-atmosphere continuum, *Physiol. Plant.*, 27(2), 161-168, <https://doi.org/10.1111/j.1399-3054.1972.tb03594.x>, 1972.

Eller, C. B., Rowland, L., Mencuccini, M., Rosas, T., Williams, K., Harper, A., Medlyn, B., Wagner, Y., Klein, T. Teodoro, G., Oliveira, R., Matos, I., Rosado, B. H. P., Fuchs, K., Wohlfahrt, G., Montagnani, L., Meir, P., Sitch, S., Cox, P.: Stomatal optimization based on xylem hydraulics (SOX) improves land surface model simulation of vegetation responses to climate. *New Phytol.*, 226. <https://doi.org/10.1111/nph.16419>, 2020.

765 Espeleta, J., West, J., and Donovan, L.: Species-specific patterns of hydraulic lift in co-occurring adult trees and grasses in a sandhill community, *Oecologia*, 138, 341-349, <https://doi.org/10.1007/s00442-004-1539-x>, 2004.

Fan, X., Hu, H., Huang, G., Huang, F., Li, Y., and Palta, J.: Soil inoculation with *Burkholderia* sp. LD-11 has positive effect on water-use efficiency in inbred lines of maize, *Plant and Soil* 390, 337-349, <https://doi.org/10.1007/s11104-015-2410-z>, 770 2015.

Farquhar, G.D., von Caemmerer, S., and Berry, J.A.: A biochemical model of photosynthetic CO<sub>2</sub> assimilation in leaves of C3 species, *Planta*, 149, 78–90, <https://doi.org/10.1007/bf00386231>, 1980.

Fu, C., Wang, G., Goulden, M.L., Scott, R.L., Bible, K., and G Cardon, Z.: Combined measurement and ~~modeling~~ modelling of the hydrological impact of hydraulic redistribution using CLM4. 5 at eight AmeriFlux sites, *Hydrol. Earth Syst. Sci.*, 20, 775 <https://doi.org/10.5194/hess-2016-24-rc1>, 2016.

Guo, Y.: Simulation of water transport in the soil-plant-atmosphere system, <https://doi.org/10.31274/rtd-180813-9473>, 1992.

Jarvis, N.: Simple physics-based models of compensatory plant water uptake: Concepts and eco-hydrological consequences, *Hydrol. Earth Syst. Sci.*, 15, 3431-3446, <https://doi.org/10.5194/hess-15-3431-2011>, 2011.

780 Jones, J.W., Hoogenboom, G., Porter, C.H., Boote, K.J., Batchelor, W.D., Hunt, L., Wilkens, P.W., Singh, U., Gijsman, A.J., and Ritchie, J.T.: The DSSAT cropping system model, *Eur. J. Agron.*, 18, 235-265, [https://doi.org/10.1016/s1161-0301\(02\)00107-7](https://doi.org/10.1016/s1161-0301(02)00107-7), 2003.

Keating, B.A., Carberry, P.S., Hammer, G.L., Probert, M.E., Robertson, M.J., Holzworth, D., Huth, N.I., Hargreaves, J.N., Meinke, H., and Hochman, Z.: An overview of APSIM, a model designed for farming systems simulation, *Eur. J. Agron.*, 18, 267-288, [https://doi.org/10.1016/s1161-0301\(02\)00108-9](https://doi.org/10.1016/s1161-0301(02)00108-9), 2003.

785 [Kennedy, D., Swenson, S., Oleson, K.W., Lawrence, D.M., Fisher, R. A., da Costa, A., and Gentine, P.: Implementing plant hydraulics in the community land model, version 5, \*J. Adv. Model. Earth Syst.\*, <https://doi.org/10.1029/2018MS001500>, 2019.](#)

Klepper, B., Rickman, R.W., and Taylor, H.M.: Farm management and the function of field crop root systems, *Agric. Water Manage.*, 7, 115–141, [https://doi.org/10.1016/0378-3774\(83\)90078-1](https://doi.org/10.1016/0378-3774(83)90078-1), 1983.

790 Krinner, G., N. Viovy, N. de Noblet-Ducoudre, J. Ogee, J. Polcher, P. Friedlingstein, P. Ciais, S. Sitch, and I. C. Prentice.: A dynamic global vegetation model for studies of the coupled atmosphere-biosphere system, *Glob. Biogeochem. Cycle*, 19 (GB1015), doi:10.1029/2003GB002199, 2005.

[Lawrence, D., Fisher, R., Koven, C., Oleson, K., Swenson, S., Vertenstein, M.: Technical Description of version 5.0 of the Community LandModel \(CLM\), 2020.](#)

795 Leitner, D., Klepsch, S., Bodner, G., and Schnepf, A.: A dynamic root system growth model based on L-Systems, *Plant Soil*, 332, 177-192, <https://doi.org/10.1007/s11104-010-0284-7>, 2010.

[Li, L., Wang YP, Yu, Q., Pak, B., Eamus, D., and Yan, J.: Improving the responses of the australian community land surface model \(cable\) to seasonal drought, \*J. Mackay, D.S., Savoy, P. R., Grossiord, C., Tai, X., Oleban, J., Wang, D., McDowell, N., Adams, H., Sperry, J. S.: Conifers depend on established roots during drought: results from a coupled model of carbon allocation and hydraulics, \*New Phytol.\*, 225\(2\), 679-692, <https://doi.org/10.1111/nph.16043>, 2019.\*](#)

800 ~~[\*Geophys. Res. Biogeosci.\*, 117\(G4\), <https://doi.org/10.1029/2012jg002038>, 2012.](#)~~

Martineau, E., Domec, J.-C., Bosc, A., Denoroy, P., Fandino, V.r.A., Lavres Jr, J., and Jordan-Meille, L.: The effects of potassium nutrition on water use in field-grown maize (*Zea mays* L.), *Environ. Exp. Bot.*, 134, 62-71, <https://doi.org/10.1016/j.envexpbot.2016.11.004>, 2017.

- 805 [Medlyn, B.E., Kauwe, M.G.D., and Duursma, R.A.: New developments in the effort to model ecosystems under water stress. \*New Phytol.\*, 212\(1\), 5-7, <https://doi.org/10.1111/nph.14082>, 2016.](https://doi.org/10.1111/nph.14082)
- [Mcdowell, N.G., Brodribb, T.J., and Nardini, A.: Hydraulics in the 21st century. \*New Phytol.\*, 224\(2\), <https://doi.org/10.1111/nph.16151>, 2019.](https://doi.org/10.1111/nph.16151)
- 810 [Mohammed, G.H., Colombo, R., Middleton, E.M., Rascher, U., Van der Tol, C., Nedbal, L., Goulas Y., Perez-Priego, O., Damm A., Meroni M., Joiner J., Cogliati S., Verhoef W., Malenovsky Z., Gastellu-Etchegorry J., Miller, J., Guanter, L., Moreno, J., Berry, J., Frankenberg, C., Zarco-Tejada, P.J.: Remote sensing of solar-induced chlorophyll fluorescence \(SIF\) in vegetation: 50 years of progress. \*Remote Sens. Environ.\*, 231, <https://doi.org/10.1016/j.rse.2019.04.030>, 2019.](https://doi.org/10.1016/j.rse.2019.04.030)
- Ning, P., Li, S., White, P.J., and Li, C.: Maize varieties released in different eras have similar root length density distributions in the soil, which are negatively correlated with local concentrations of soil mineral nitrogen, *PLOS one*, 10, e0121892, <https://doi.org/10.1371/journal.pone.0121892>, 2015.
- 815 [Niu, G., Fang, Y., Chang, L., Jin, J., Yuan, H., and Zeng, X.: Enhancing the Noah-MP ecosystem response to droughts with an explicit representation of plant water storage supplied by dynamic root water uptake, \*J. Adv. Model. Earth Syst.\*, <https://doi.org/10.1029/2020MS002062>, 2020.](https://doi.org/10.1029/2020MS002062)
- O'Toole, J.C., and Cruz, R.T.: Response of leaf water potential, stomatal resistance, and leaf rolling to water stress, *Plant Physiol.*, 65, 428-432, <https://doi.org/10.1104/pp.65.3.428>, 1980.
- 820 [Oikeh, S., Kling, J., Horst, W., Chude, V., and Carsky, R.: Growth and distribution of maize roots under nitrogen fertilization in plinthite soil, \*Field Crop. Res.\*, 62, 1-13, \[https://doi.org/10.1016/s0378-4290\\(98\\)00169-5\]\(https://doi.org/10.1016/s0378-4290\(98\)00169-5\), 1999.](https://doi.org/10.1016/s0378-4290(98)00169-5)
- Peng, Y., Yu, P., Zhang, Y., Sun, G., Ning, P., Li, X., and Li, C.: Temporal and spatial dynamics in root length density of field-grown maize and NPK in the soil profile, *Field Crop. Res.*, 131, 9-16, <https://doi.org/10.1016/j.fcr.2012.03.003>, 2012.
- 825 [Qin, R., Stamp, P., and Richner, W.: Impact of tillage on maize rooting in a Cambisol and Luvisol in Switzerland, \*Soil Tillage Res.\*, 85, 50-61, <https://doi.org/10.1016/j.still.2004.12.003>, 2006.](https://doi.org/10.1016/j.still.2004.12.003)
- Reichstein, M., Falge, E., Baldocchi, D., Papale, D., Aubinet, M., Berbigier, P., Bernhofer, C., Buchmann, N., Gilmanov, T., and Granier, A.: On the separation of net ecosystem exchange into assimilation and ecosystem respiration: review and improved algorithm, *Glob. Change Biol.*, 11, 1424-1439, <https://doi.org/10.1111/j.1365-2486.2005.001002.x>, 2005.
- 830 [Reid, J.B., and Huck, M.G.: Diurnal variation of crop hydraulic resistance: a new analysis. \*Agron. J.\*, 82, 827-834, \[https://doi.org/10.1016/0378-3774\\(90\\)90029-X\]\(https://doi.org/10.1016/0378-3774\(90\)90029-X\), 1990.](https://doi.org/10.1016/0378-3774(90)90029-X)

- Richards, J.H. and Caldwell, M.M.: Hydraulic lift: substantial nocturnal water transport between soil layers by *Artemisia tridentata* roots, *Oecologia*, 73, 486-489, <https://doi.org/10.1007/bf00379405>, 1987.
- Robertson, M., Fukai, S., Hammer, G., and Ludlow, M.: Modelling root growth of grain sorghum using the CERES approach, *Field Crop. Res.*, 33, 113-130, [https://doi.org/10.1016/0378-4290\(93\)90097-7](https://doi.org/10.1016/0378-4290(93)90097-7), 1993.
- 835 Ryel, R., Caldwell, M., Yoder, C., Or, D., and Leffler, A.: Hydraulic redistribution in a stand of *Artemisia tridentata*: evaluation of benefits to transpiration assessed with a simulation model, *Oecologia*, 130, 173-184, <https://doi.org/10.1007/s004420100794>, 2002.
- Schroder, J., Groenwold, J., and Zaharieva, T.: Soil mineral nitrogen availability to young maize plants as related to root length density distribution and fertilizer application method, *NJAS-Wagen. J. Life Sci.*, 44, 209-225, 1996.
- 840 Seneviratne, S.I., Corti, T., Davin, E. L., Hirschi, M., Jaeger, E., B., L., I., Orlowsky, B., and Teuling A. J.: Investigating soil moisture-climate interactions in a changing climate: a review, *Earth-Sci. Rev*, 99, 125–161, <https://doi.org/10.1016/j.earscirev.2010.02.004>, 2010.
- [Shan, N., Ju, W., Migliavacca, M., Martini, D., Guanter, L., and Chen, J.M., Goulas, Y., Zhang, Y.: Modeling canopy conductance and transpiration from solar-induced chlorophyll fluorescence, \*Agric. For. Meteorol.\*, 268, 189-201, <https://doi.org/10.1016/j.agrformet.2019.01.031>, 2019.](https://doi.org/10.1016/j.agrformet.2019.01.031)
- 845 <https://doi.org/10.1016/j.agrformet.2019.01.031>, 2019.
- Stöckle, C.O., Donatelli, M., and Nelson, R.: CropSyst, a cropping systems simulation model, *Eur. J. Agron.*, 18, 289-307, [https://doi.org/10.1016/s1161-0301\(02\)00109-0](https://doi.org/10.1016/s1161-0301(02)00109-0), 2003.
- [Sun, Y., Fu, R., Dickinson, R., Joiner, J., Frankenberg, C., Gu, L., Xia, Y., Fernando, N.: Drought onset mechanisms revealed by satellite solar-induced chlorophyll fluorescence: insights from two contrasting extreme events, \*J. Geophys. Res.-Biogeosci.\*, 120\(11\), 2427-2440, <https://doi.org/10.1002/2015JG003150>, 2016.](https://doi.org/10.1002/2015JG003150)
- 850 <https://doi.org/10.1002/2015JG003150>, 2016.
- Supit, I., Hooijer, A., and Van Diepen, C.: System description of the WOFOST 6.0 crop simulation model implemented in CGMS, vol. 1: Theory and Algorithms, Joint Research Centre, Commission of the European Communities, EUR 15956, 146, 1994.
- Van Dam, J.C.: Field-Scale Water Flow and Solute Transport. SWAP Model Concepts, Parameter Estimation and Case Studies, 855 Wageningen University, Wageningen, The Netherlands, pp. 167, 2000.
- Van der Tol, C., Verhoef, W., Timmermans, J., Verhoef, A., and Su, Z.: An integrated model of soil-canopy spectral radiances, photosynthesis, fluorescence, temperature and energy balance, *Biogeosciences*, 6, 3109-3129, <https://doi.org/10.5194/bg-6-3109-2009>, 2009.

- 860 [Van der Tol, C., Berry, J., Campbell, P., Rascher, U.: Models of fluorescence and photosynthesis for interpreting measurements of solar-induced chlorophyll fluorescence, J. Geophys. Res.-Biogeosci., 119, 2312–2327, doi:10.1002/2014JG002713, 2014.](#)
- Van Genuchten, M.T.: A closed-form equation for predicting the hydraulic conductivity of unsaturated soils, Soil Sci. Soc. Am. J., 44, 892–898, <https://doi.org/10.2136/sssaj1980.03615995004400050002x>, 1980.
- Wang, E. and Smith, C.J.: Modelling the growth and water uptake function of plant root systems: a review, Aust. J. Agr. Res., 865 55, 501-523, <https://doi.org/10.1071/ar03201>, 2004.
- ~~Wang, Y., Cai, HJ., Yu, LY., Peng XB., Xu JT., and Wang XW.: Evapotranspiration partitioning and crop coefficient of maize in dry semi-humid climate regime, Agric. Water Manage[preprint], 236, <https://doi.org/10.1016/j.agwat.2020.106164>, 2020.~~
- 870 ~~Wang, Y., Cai, HJ.,~~ Zeng, YJ., Su, Z., and Yu, LY.: Data underlying the research on Seasonal and interannual variation in evapotranspiration, energy flux, and Bowen ratio over a dry semi-humid cropland in Northwest China, 4TU. Centre for Research Data. Dataset, <https://doi.org/10.4121/uuid:aa0ed483-701e-4ba0-b7b0-674695f5f7a7>, 2019.
- Wang, Y., [Cai, HJ., Yu, LY., Peng XB., Xu JT., and Wang XW.: Evapotranspiration partitioning and crop coefficient of maize in dry semi-humid climate regime, Agric. Water Manage\[preprint\], 236, <https://doi.org/10.1016/j.agwat.2020.106164>, 2020a.](#)
- 875 [Wang, Y., Zeng, YJ., Yu, LY., Yang P., Van der Tol C., Su, Z., and Cai, HJ.: Integrated ModelingModelling of Photosynthesis and Transfer of Energy, Mass and Momentum \(SCOPE\\_STEMMUS-SCOPE v1.0\), Zenodo, <https://doi.org/10.5281/zenodo.3839092>, 20202020b.](#)
- Wiesler, F. and Horst, W.: Root growth and nitrate utilization of maize cultivars under field conditions, Plant Soil, 163, 267-277, <https://doi.org/10.1007/bf00007976>, 1994.
- Williams, J., Jones, C., Kiniry, J., and Spanel, D.A.: The EPIC crop growth model. Transactions of the ASAE, 32, 497-0511, <https://doi.org/10.13031/2013.31032>, 1989.
- 880 Williams, J.R., Gerik, T., Francis, L., Greiner, J., Magre, M., Meinardus, A., Steglich, E., and Taylor, R.: EPIC – Environmental Policy Integrated Climate Model – UsersManual version 0810, Blackland Research and Extension Center – Texas A&MAgriLife, Temple, TX, 2014.
- 885 [Williams, M., Rastetter, E. B., Fernandes, D.N., Goulden, M. L., Wofsy, S.C., Shaver G.R., Melillo J.M., Munger, J.W., Fan, S.M., and Nadelhoffer, K. J.: Modelling the soil-plant-atmosphere continuum in a Quercus-Acer stand at Harvard Forest: the regulation of stomatal conductance by light, nitrogen and soil/plant hydraulic properties, Plant Cell Environ., 19\(8\), 911-927, <https://doi.org/10.1111/j.1365-3040.1996.tb00456.x>, 1996.](#)

- Wu, L., McGechan, M., Watson, C., and Baddeley, J.: Developing existing plant root system architecture models to meet future agricultural challenges, *Adv. Agron.*, 85, 85004-85001, [https://doi.org/10.1016/s0065-2113\(04\)85004-1](https://doi.org/10.1016/s0065-2113(04)85004-1), 2005.
- Xu, L. and Baldocchi, D. D.: Seasonal trends in photosynthetic parameters and stomatal conductance of blue oak (*Quercus douglasii*) under prolonged summer drought and high temperature, *Tree Physiol.*, 23(13), 865-877, <https://doi.org/10.1093/treephys/23.13.865>, 2003.
- [Xu, X., Medvigy, D., Powers, J.S., Becknell, J.M., and Guan, K.: Diversity in plant hydraulic traits explains seasonal and inter-annual variations of vegetation dynamics in seasonally dry tropical forests, \*New Phytol.\*, 212\(1\), <https://doi.org/10.1111/nph.14009>, 2016.](https://doi.org/10.1111/nph.14009)
- 895 Yu, L., Zeng, Y., Su, Z., Cai, H., and Zheng, Z.: The effect of different evapotranspiration methods on portraying soil water dynamics and ET partitioning in a semi-arid environment in Northwest China, *Hydrol. Earth Syst. Sci.*, 20, 975-990, <https://doi.org/10.5194/hess-20-975-2016>, 2016.
- Yu, L., Zeng, Y., Wen, J., and Su, Z.: Liquid-Vapor-Air Flow in the Frozen Soil, *J. Geophys. Res.-Atmos.*, 123(14), 7393-7415, <https://doi.org/10.1029/2018jd028502>, 2018.
- 900 Zeng, Y., Su, Z., Wan, L., and Wen, J.: A simulation analysis of the advective effect on evaporation using a two-phase heat and mass flow model, *Water Resour. Res.*, 47(10), W10529, <https://doi.org/10.1029/2011wr010701>, 2011a.
- Zeng, Y., Su, Z., Wan, L., and Wen, J.: Numerical analysis of air-water-heat flow in unsaturated soil: Is it necessary to consider airflow in land surface models?, *J. Geophys. Res.-Atmos.*, 116(D20), D20107, <https://doi.org/10.1029/2011jd015835>, 2011b.
- Zeng, Y. and Su, Z.: STEMMUS: Simultaneous Transfer of Energy, Mass and Momentum in Unsaturated Soil, University of  
905 Twente, Faculty of Geo-Information and Earth Observation (ITC), Enschede, 2013.
- [Zhang, Y., Guanter, L., Joiner, J., Song, L., and Guan, K.: Spatially-explicit monitoring of crop photosynthetic capacity through space-based chlorophyll fluorescence data, \*Remote Sens. Environ.\*, 210, 362-374, <https://doi.org/10.1016/j.rse.2018.03.031>, 2018.](https://doi.org/10.1016/j.rse.2018.03.031)
- [Zhang, Z., Zhang, Y.G., Porcar-Castell, A., Joiner, J., Guanter, L., Yang, X., Migliavacca, M., Ju, W., Sun, Z., Chen, S., Martini, D., Zhang, Q., Li, Z., Cleverly, J., Wang, H., and Goulas, Y.: Reduction of structural impacts and distinction of photosynthetic pathways in a global estimation of GPP from space-borne solar-induced chlorophyll fluorescence, \*Remote Sens. Environ.\*, 111722, <https://doi.org/10.1016/j.rse.2020.111722>, 2020.](https://doi.org/10.1016/j.rse.2020.111722)
- Zheng, Z. and Wang, G.: ModelingModelling the dynamic root water uptake and its hydrological impact at the Reserva Jaru site in Amazonia, *J. Geophys. Res.-Biogeosci.*, 112, <https://doi.org/10.1029/2007jg000413>, 2007.

915 Zhou, S., Duursma, R.A., Medlyn, B.E., Kelly, J.W., and Prentice, I.C.: How should we model plant responses to drought? An analysis of stomatal and non-stomatal responses to water stress, *Agric. For. Meteorol.*, 182, 204-214, <https://doi.org/10.1016/j.agrformet.2013.05.009>, 2013.

Zhou, S., Yu B., Huang Y., and Wang G.: The effect of vapor pressure deficit on water use efficiency at the subdaily time scale, *Geophys. Res. Lett.*, 41, 5005–5013, doi:10.1002/2014GL060741, 2014.

920 Zhou, S., Yu, B., Zhang, Y., Huang, Y., and Wang, G.: Partitioning evapotranspiration based on the concept of underlying water use efficiency, *Water Resour. Res.*, 52, 1160-1175, <https://doi.org/10.1002/2015wr017766>, 2016.

Zhu, S., Chen, H., Zhang, X., Wei, N., Shanguan, W., Yuan, H., Zhang, S., Wang, L., Zhou, L., and Dai, Y. Incorporating root hydraulic redistribution and compensatory water uptake in the Common Land Model: Effects on site level and global land ~~modeling~~, ~~modelling~~. *J. Geophys. Res.-Atmos.*, 122, 7308-7322, <https://doi.org/10.1002/2016jd025744>, 2017.

925 Zhuang, J., Nakayama, K., Yu, G.-R., and Urushisaki, T.: Estimation of root water uptake of maize: an ecophysiological perspective, *Field Crop. Res.*, 69, 201-213, [https://doi.org/10.1016/s0378-4290\(00\)00142-8](https://doi.org/10.1016/s0378-4290(00)00142-8), 2001a.

Zhuang, J., Yu, G., and Nakayama, K.: Scaling of root length density of maize in the field profile, *Plant Soil*, 235, 135-142, <https://doi.org/10.1023/A:1011972019617>, 2001b.